Ecohydrology

WILEY

SPECIAL ISSUE PAPER OPEN ACCESS

Elementary Mathematics Helps to Shed Light on the Transpiration Budget Under Water Stress

Concetta D'Amato[1,2] | Riccardo Rigon[1,2]

[1]C3A–Center Agriculture Food Environment, University of Trento, San Michele all'Adige, Italy | [2]Department of Civil, Environmental and Mechanical Engineering, University of Trento, Trento, Italy

Correspondence: Riccardo Rigon (riccardo.rigon@unitn.it)

Received: 2 January 2024 | **Revised:** 25 January 2025 | **Accepted:** 13 February 2025

Funding: This paper has been supported by MIUR Project (PRIN 2020) "Unravelling interactions between WATER 380 and carbon cycles during drought and their impact on water resources and forest and grassland ecosySTEMs in the Mediterranean climate (WATERSTEM) " (protocol code: 20202WF53Z) and "WAFER" @CNR projects (Consiglio Nazionale delle Ricerche).

Keywords: conductances in soil–plant–atmosphere interactions | energy and water budgets | Penman–Monteith | plants hydraulics | transpiration modelling | water limited transpiration

ABSTRACT

This paper aims to present a methodology for accurately describing transpiration by employing appropriate physical equations. While some simplifications have been made, including the use of a simplified treatment of turbulence and the neglect of the thermal capacity of transpiring leaves, it is argued that the chosen scheme has general validity in identifying the primary mechanisms governing transpiration. To achieve this objective, a traditional treatment involving five equations, including the mass budget, is used. Initially, a simplified approach that does not consider the water budget is introduced to outline the general procedure to explicitly address canopies. Subsequently, the water budget is incorporated to appropriately account for water stress in transpiration. In this context, a novel linearisation of the extended Clausius–Clapeyron equation, incorporating the Kelvin effect, is employed. It is demonstrated that the well-known Penman formula emerges as one of the solutions within a system of equations, providing estimates for temperature (T), vapor content in air (e) and the thermal transport of heat (H). The method, initially conceived for homogeneous canopies, is expanded to encompass sun–shade canopy layers. By employing the water mass balance, the trade-off between atmospheric evaporation demand and the water delivery capacity of the soil and stem is elucidated. Notably, it is revealed that the pressure potential within leaves is not solely determined by capillarity, but rather represents the dynamic outcome of the intricate interactions within the soil–plant–atmosphere continuum. These findings highlight differences from more simplistic approaches commonly employed, particularly concerning canopies. Overall, this study presents a methodological framework to accurately describe transpiration, incorporating key equations and addressing the complex dynamics involved in the soil–plant–atmosphere continuum, and suggests various directions of research in the field.

1 | Introduction

Transpiration plays an important role in the hydrological cycle, accounting for an estimated 30% to 60% of the total water budget, depending on the location (Abera, Formetta, Borga, et al. 2017; Abera, Formetta, Borga, et al. 2017). However, quantifying transpiration accurately can be challenging due to uncertain measurements and models (Mauder, Foken, and Cuxart 2020). In practical applications, semi-empirical formulations are commonly employed, but their underlying rationale and limitations are not fully understood by practitioners, particularly in traditional engineering hydrology, where the complexities of the soil–plant–atmosphere continuum (SPAC) are often overlooked (Lawrence Dingman 2015; Jovanovic and Israel 2012).

Although some researchers have adopted simplified models programmatically to gain an overview of the interactions within the SPAC and explore the ecohydrological dynamics at hillslope and larger spatial scales (Eagleson 1978; Rodriguez-Iturbe and Porporato 2007; Daly, Porporato, and Rodriguez-Iturbe 2004a), further progress in understanding transpiration required moving beyond idealised models. This epistemological shift, or de-idealisation (Cassini 2021), is crucial to obtain specific answers and compare them with experimental data, particularly for distinguishing the behaviour of individual plants or stands, which is influenced by various factors such as radiation, atmospheric conditions and soil water potential (Porporato and Yin 2022). Physiological and phenological adaptations enable plants to optimise growth, and the concept of optimality has been invoked in various aspects of the photosynthetic-transpiration process. This includes the optimality of the water cycle in the context of ecological webs (Eagleson 2005; Rodriguez-Iturbe and Porporato 2007; Rodriguez-Iturbe 2000), the optimal adaptation of the plant xylem to ensure uniform water distribution throughout the canopy (Soriano et al. 2020) and the optimal photosynthesis theory (Cowan and Farquhar 1977; Katul, Palmroth, and Oren 2009; Medlyn et al. 2011) reviewed in Dewar et al. (2018) and Joshi et al. (2022).

A robust foundation for the investigation of such complex topics can be established on the basis of the principles of energy and mass conservation, employing a 'constructive' approach that incrementally introduces complexity only as needed. While this may involve a system of coupled partial differential equations such as Navier–Stokes, heat and water vapor advection–dispersion (Monson and Baldocchi 2014) and Richards equations (Tubini and Rigon 2022), it would be preferable to avoid obscuring physical and physiological insights with numerical complexities. The objective of this paper is to prioritise the capture of essential system interactions through the use of a simplified, explicitly tractable framework. This approach is designed to clarify key physical processes and to establish a foundation for the development of more complex models in the future.

Overall, this paper aims to provide modellers with a blueprint for developing SPAC hydraulic models of increasing complexity, potentially integrating water, energy and carbon cycle budgets, as needed by sophisticated laboratory setup (Werner et al. 2021, 2024). Our approach emphasises a thoughtful progression from simplicity, and each added feature was carefully evaluated for the trade-offs between complexity and model tractability. Thus, we pay careful attention to the mathematical derivation to clarify our methodology and make it more explicit.

While many aspects we address are known, they have not been cohesively treated. For instance, the recent work by Porporato and Yin (2022) does not cover what we discuss in Sections 4–6. Although the topics related to conductance are addressed, for instance, in Bonan (2019), there is no clear guiding principle to introduce these topics as a hierarchy of choices. Similarly, Monson and Baldocchi (2014) cover the relevant aspects but not those specifically related to modeling. None of the aforementioned references adequately address nonstomatal behaviours. Insightful reviews like Tyree and Ewers (1991), and more recent ones as Venturas, Sperry, and Hacke (2017) and Lehnebach et al. (2018), offer valuable physiological information but lack the mathematical depth needed for quantitative hydrological modeling. This limits their utility for hydrologists aiming to implement SPAC models with a proper understanding of the underlying processes.

Therefore, the starting point of this paper is a critical adoption of the Penman-Monteith (PM) equation derivation. Section 2 presents this derivation in a revised extension, following the approach of Schymanski and Or (2017), and addresses canopies through the integration of a reliable radiation treatment, based on de Pury and Farquhar (1997) and Ryu et al. (2011).

In Section 3, we examine transpiration conductance, as the explicit or implicit dependence of conductance on air temperature can affect the solutions of the coupled transport and energy budgets.

However, PM does not account for the water budget (Bottazzi 2020) and introduces a bias in the transpiration estimates when plants face limited water availability. This omission has been historically corrected using empirical formulations for conductances, or stress factors (Bonan 2019; Monson and Baldocchi 2014), which evolved to include both physiological feedback and limiting environmental factors. While these formulations may have been effective, in Section 4, we propose that explicitly incorporating the water budget, that is, plants hydraulics, better clarify the physical and physiological processes involved in transpiration.

Applying the mass budget, we find that water supply to plants is limited by the decreasing pressure values inside xylem and leaves due to increasing embolism, counteracted by the closure of the stomata (Sperry, Stiller, and Hacke 2003). With the possible exception of Vesala et al. (2017), most of the literature does not deal properly with these two concurrent actions introducing distortions into the description of the transpiration phenomenon and in parameter estimation, which, in Section 4 we suggest to correct.

Section 5 demonstrates explicitly how the inclusion of the water budget can be performed. In Section 6, we discuss conditions under which the more physically accurate sun–shade model (de Pury and Farquhar 1997; Wang and Leuning 1998) can be solved under additional assumptions.

In the final Sections 7 and 8, we present discussion and conclusions, which address the open questions that our approach raises.

The paper also includes appendices with a detailed derivation of the energy budget for unit leaf area and discussions on parameterising hydraulic conductivity in plants.

2 | Plant Transpiration in Revised Big-Leaf/Penman-Like Approach

To clarify our approach to estimating transpiration, we begin by introducing the big-leaf approximation. This method assumes that the entire canopy can be represented by its average properties and treated as a single, homogeneous layer, characterised by

parameters such as leaf area index (L_c), that is, the total leaf area per unit ground surface area, stomatal conductance and photosynthesis rates (Deardorff 1978; Monteith 1981). This approach dates back to Penman and Keen (1948) and Monteith (1981), and one of its treatments can be found in Schymanski and Or (2017). In the following, L_c is considered a measured variable representing the canopy surface area per unit of projected ground area. By explicitly accounting for it, our derivation of the Penman–Monteith equation differs slightly from the treatments typically found in textbooks, such as Porporato and Yin (2022) and Brutsaert (2023).

Although our derivation looks straightforward and familiar, it serves an essential role by introducing key concepts: the role of canopies, the distinction between conductance factors for water vapor and sensible heat transport and the inclusion of canopy radiation emission. The derivation itself clarifies the methodology we use in subsequent sections, where we further extend our results

The starting point for our derivation is the energy balance equation, where thermal capacity is neglected, along with the transport equations for temperature and water vapor and the Clausius–Clapeyron equation. As shown by Schymanski and Or (2017), these represent a system of four equations with four unknowns that can be solved straightforwardly. The equations are listed and discussed in detail below organised in reverse order for sake of clarity.

- The Clausius–Clapeyron equation

The equation captures the relationship between the saturation vapor pressure and temperature, providing the thermodynamical basis for understanding the presence of water vapor in the system (Bohren and Albrecht 1998):

$$e^*(T) = e_0^*(T_0) e^{-\frac{\lambda m_{H_2O}}{R}\left(\frac{1}{T}-\frac{1}{T_0}\right)} \tag{1}$$

where e^* (Pa) is the water vapor tension at temperature T; $e_0^* = 611$ (Pa)is the water vapor pressure at the reference temperature $T_0 = 273.15$ (K); $\lambda = 2.26 \times 10^6$ (J kg^{-1}) is the enthalpy of vaporisation of water; $R = 8.3144$ is the universal gas constant (J k^{-1} mol^{-1}); $m_{H_2O} = 18.01528$ (kg mol^{-1}) is the molar mass of water and T (K) is the absolute temperature. All the symbols are summarised for readers' convenience in Table A1 of Appendix A. In this study, Equation (1) accounts for water vapor generation and will be assumed to hold instantaneously in the vicinity of liquid water under free thermodynamic conditions.

- The transport of water vapor into the atmosphere

The equation we use below, as well as the companion equation for the sensible heat transport, originates from the works of Porporato and Yin (2022) and is justifiable under simplified landscape geometries. It reads as follows:

$$E_T = C_E L_c \frac{\xi}{p}(e_l - e_a) := C_E L_c \frac{\xi}{p} e_\Delta \tag{2}$$

where C_E is the transpiration conductance which captures much of the complexity of the transport processes and may include corrections for atmospheric stability conditions and is detailed in the next section; e_l (Pa) is the water vapor pressure at the leaf surface, and e_a (Pa) is the water vapor pressure in the atmosphere; L_c (-) is the leaf area index of the whole canopy; $\xi = 0.622$ (-) is the ratio between the dry and wet air gas constants; p (Pa) is the atmospheric pressure. To simplify subsequent manipulations, the pressure gap between leaf and air, $e_\Delta := (e_l - e_a)$, has also been defined. We introduce the idealised hypothesis that all leaves of a canopy transpire equally. The equation obviously returns null transpiration in the absence of a canopy.

- The transport of thermal energy (sensible heat) by turbulence is as follows:

$$H = 2Cf(L_c)(T_l - T_a) := 2Cf(L_c)T_\Delta \tag{3}$$

where the factor "2" is required because leaves exchange heat from their two sides; $C = \rho_a \widehat{C} c_p \bar{u}$ (m s^{-1}) is the heat transport conductance, as derived for instance in Brutsaert (1982) and Banerjee, De Roo, and Mauder (2017), with ρ_a being the air density, $\widehat{C}$ a dimensionless conductance derived from the analysis of the turbulent behaviour in proximity of the leaves, c_p (J kg^{-1} K^{-1}) the thermal capacity of air, and $\bar{u}$ (m s^{-1}) the module of the mean horizontal wind velocity; T_l (°K) is the leaf temperature, and T_a (K) is the air temperature. To simplify the notation, the temperature gap, $T_\Delta := (T_l - T_a)$, has also been defined.

Equation (3) returns a null sensible heat exchange in the absence of a canopy. The function $f(L_c)$ describes how the canopy acts as a thermal radiator. If we consider $f(L_c) = \min(L_c, 1)$, this would mean that when $L_c > 1$, the canopy behaves as a single layer (with heat exchange surfaces at the top and bottom) and the effects of the multiplicity of leaves are neglected. A greater efficiency in dissipating heat can be properly characterised after appropriate studies, such as those in Muller et al. (2021) and Banerjee, De Roo, and Mauder (2017), which include the possibility of a strong coupling of conductances/resistances with atmospheric instability. The paper by Liu et al. (2007) offers a comprehensive list of parameterisations that could be used for this scope. The maximum efficiency of thermal dissipation is obtained when each leaf dissipates as if it were not exchanging heat with the other leaves and, in this case, $f(L_C) = L_c$.

It is important to note that Equations (2) and (3) provide a simplified representation of the complex mixing processes that occur at the surface layer. However, they can be viewed as a zeroth-order approximation that is useful for practical purposes. Given their simplicity, these equations allow for the problem to be treated without relying on complicated numerical methods while also retaining the core causal relations between the hydrological quantities and the thermodynamic driving forces.

- The stationary energy budget with radiation emission from canopy

The energy budget in the big-leaf approach is represented in Figure 1. All the leaves in the canopy are treated in the same way, and it is assumed that they share the same values for any of the variables involved in the budget. The Extended Petri Nets diagram (EPN) in (Bancheri, Serafin, and Rigon 2019) Figure 1 represents the budget inputs and outputs (as squares) and the

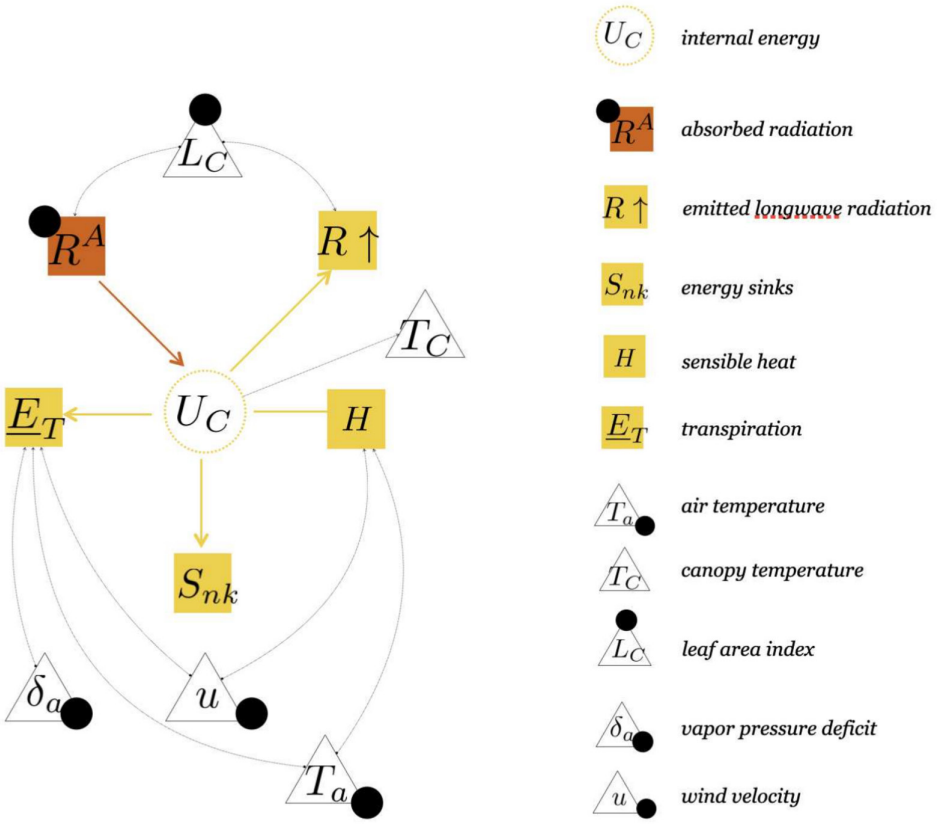

FIGURE 1 | The figure illustrates the extended petri net (EPN) depicting the energy budget interactions at the plant scale, as described in the text. In the diagram, the circles represent the energy storage, while squares represent fluxes to and from the storage. The budget is noncapacitive, meaning that changes in the boundary conditions instantaneously affect the water state within the plant compartments (this characteristic being indicated by representing the energy storage circle in dashed). Triangles represent variables that control the fluxes, which can be either derived from the state variables controlling the storage or regulated by external/environmental conditions. Black dots mark quantities that are supposed to be given as known time series. The internal energy of the plant system (U_C) is determined by the radiation fluxes ($R\downarrow$), from which the longwave radiation emitted by the plant ($R\uparrow$) is subtracted. Transpiration (E_T) and the exchange of thermal energy (sensible heat) with the atmosphere (H) represent the energy exchanged through turbulent transfer. Additionally, various transformations of the received energy are represented by S_{nk}, including the storage of chemical energy used to form the plant's structure, leaves and fruits. The variables controlling the energy budget include the canopy leaf area index (L_C), wind velocity (u) and the temperature of the canopy, which is a byproduct of the plant's internal energy (U_C) and the water vapor deficit of the air, δ_a, itself a function of the air temperature, T_a, but added here separately for completeness.

energy variation (as circles). Triangles with arrows exiting from the circle indicate variables that are affected by the energy content of the system and triangles with arrows entering the squares indicate variables that controls the fluxes, like the leaf area index controlling radiation and the air temperature controlling the transpiration flux.

This budget is firstly composed by the radiation input that can be expressed, for instance (de Pury 1995), as follows:

$$R^A = R_b(0)(1-\alpha_b)\left(1-e^{-k'_b Lc}\right) + R_d(0)(1-\alpha_d)\left(1-e^{-k'_d Lc}\right) \quad (4)$$

where R^A is the radiation absorbed by the canopy; $R_b(0)$ is the direct sunlight at the top of the canopy; α_b is the albedo for the direct solar radiation; k'_b is an extinction coefficient for the direct solar beam; L_c is the total leaf area index of the canopy; and the quantities with subscript d are the analogous ones for the diffuse radiation. Radiation contributions are null when the leaves are not present and $L_c = 0$ (for more details, see Appendix B).

With the above specifications, the energy budget for the bulk canopy, as represented in Figure 1, reads as follows:

$$R^A - 2L_c \underbrace{\epsilon\sigma T_l^4}_{R_\uparrow} = H + b\lambda E_T + L_c S_{nk} \quad (5)$$

where H (Wm^{-2}) (as in Equation 3) is the thermal energy exchanged via turbulence between the plant and the atmosphere and E_T (as in Equation 2) is the transpiration from vegetation. In this formulation, it is assumed that the internal state of the canopy, that is, its T_l, changes when the radiation fluxes change, but the adaptation to match the inputs is instantaneous. The triangles in the EPN are referred to as 'controllers' of the budget, which are the quantities that regulate the energy fluxes.

The term S_{nk} represents an energy sink that can account for the energy absorbed by photosynthetic processes, which is typically neglected due to its relatively small magnitude. However, we retain it for its conceptual significance and as a placeholder for other potential energy sinks that may be relevant in specific cases, providing greater flexibility in the model. The term U_C representing the internal energy in Figure 1 is not present in the equation because it is considered instantaneously adapting to the input and the output, meaning that the thermal capacity of the canopy is neglected and $\partial U_C/\partial dt = 0$.

The parameter b is $b = 1$ for epistomatous leaves (which have stomata on one side) and $b = 2$ for amphystomatous leaves (which have stomata on two sides). The numeric factor '2' in front of the radiative feedback appears because, as seen with Equation (3), leaves exchange thermal energy through both their sides. The presence of radiation canopy emission, $R\uparrow$, serves to prevent the leaves from reaching excessive temperatures (Bottazzi 2020) and to maintain them within the natural range (Bernacchi et al. 2009; Gabriel 2021).

In Equations 1,2,3,5, the water budget is missing, which means that our system is not water limited, that is, water free to evaporate is thought to be always available. The unknown variables in Equation (5) are as follows: E_T, e_l, T_l and H. Therefore, to find them, we need all four equations.

Before manipulating the equations to find the solutions of the system, we consider the Taylor expansion of Equation (1) around the air temperature, as suggested by Penman and Keen (1948):

$$e^*(T_l) = e_a^* + \Delta\Big|_{T_a} T_\Delta + O(\Delta T_a^2) \tag{6}$$

where e_a^* is the vapor tension in air, $\Delta\Big|_{T_a}$ is the derivative of the Clausius–Clapeyron equation (Equation 1) estimated at the air temperature T_a, and $O(\Delta T^2)$ are terms of the Taylor's expansion higher than 1. For the sake of notational simplicity, in the following, we will denote $\Delta\Big|_{T_a}$ as Δ, the slope of the water saturation curve without any further specification. That is to say,

$$\Delta\Big|_{T_a} \equiv \Delta := \frac{\lambda m_{H_2O}}{R}\frac{1}{T_a^2} e_0^* e^{-\frac{\lambda m_{H_2O}}{R}\left(\frac{1}{T_a}-\frac{1}{T_0}\right)} \tag{7}$$

where all the quantities have been previously specified.

The e_Δ can be further decomposed in terms of the vapor pressure deficits close to the leaf and in the air:

$$\begin{aligned} e_\Delta: \quad &= (e_l - e_a) = (e_l - e_l^* + e_l^* - e_a) \approx \\ &-\delta_l + e_a^* + \Delta T_\Delta - e_a = \delta_a - \delta_l + \Delta T_\Delta \end{aligned} \tag{8}$$

where the "$*$" indicates water vapor tension quantities to be estimated by the Clausius–Clapeyron equation, the quantities labelled with "l" are those relative to the leaves and those marked with the subscript a are relative to the air.

In this way, the pressure gap becomes a function of the temperature gap, T_Δ, and the vapor pressure deficits, δ_a and δ_l. The latter, in turn, are functions of the air temperatures (measured) and temperature of the leaves (unknown). Therefore, there is a dependence of e_Δ on the temperatures of the leaves. The hypothesis actually made by Penman and Keen (1948) was $\delta_l = 0$, which means that in the stomata, the vapor is at "saturation" pressure. Under this hypothesis, we have reduced the unknowns to three because the atmospheric water pressure deficit, δ_a is known, depending on the measured e_a and T_a. For a simple solution of the system, only one obstacle remains: the term $\epsilon\sigma T_l^4$, which is nonlinear. However, as in Bottazzi (2020), it can be conveniently linearised by approximating it as follows:

$$R\uparrow = \epsilon\sigma T_l^4 = \epsilon\sigma T_a^3 T_l := \epsilon\sigma T_a^3 (T_l - T_a + T_a) = \epsilon\sigma T_a^3 T_\Delta + \epsilon\sigma T_a^4 \tag{9}$$

Having used this finite difference type of approximation, Equation (5) is linear in the temperature gap, and the system of Equations (2), (3) and (5) can be solved easily in terms of the supposedly known variables, i.e., $\bar{u}$, δ_a, T_a, and R_n (drawn as 'controllers' in Figure 1).

Substituting the expressions of the terms derived from Equations (2), (3) and (6) into Equation (5) results in the following:

$$T_\Delta = \frac{R^A - b\lambda L_c C_E \frac{\xi}{p}\delta_a - L_c S_{nk} - 2L_c\epsilon\sigma T_a^4}{2Cf(L_c) + b\lambda C_E L_c \frac{\xi}{p}\Delta + 2L_c\epsilon\sigma T_a^3} \tag{10}$$

The result simplifies when $f(L_c) = 1$ and R_A is assumed to be proportional to L_c. In this case, L_c cancels out, but the solution still differs from the standard Penman derivation because the sink term and canopy radiation emission are included, which are not accounted for in the original formulation. As a result, the solution shows that $T_\Delta \neq 0$, even in the simplified cases where the energy sinks are null and the radiative response of leaves is neglected. It is easy to observe that any increase in the conductance C_E decreases the temperature gap and, also, the higher the air temperature, the lower the temperature gap. The thermal energy exchange is simple to estimate by substituting Equation (10) into Equation (3) as follows:

$$H = 2Cf(L_c)\frac{R^A - b\lambda L_c C_E \frac{\xi}{p}\delta_a - L_c S_{nk} - 2L_c\epsilon\sigma T_a^4}{2Cf(L_c) + b\lambda C_E L_c \frac{\xi}{p}\Delta + 2L_c\epsilon\sigma T_a^3} \tag{11}$$

In turn, Equation (10) substituted in Equation (8) gives the following:

$$\begin{aligned} e_\Delta \quad &= \frac{2Cf(L_c) + 2L_c\epsilon\sigma T_a^3}{2Cf(L_c) + b\lambda C_E L_c \frac{\xi}{p}\Delta + 2L_c\epsilon\sigma T_a^3}\delta_a \\ &+ \frac{R^A - L_c S_{nk} - 2L_c\epsilon\sigma T_a^4}{2Cf(L_c) + b\lambda C_E L_c \frac{\xi}{p}\Delta + 2L_c\epsilon\sigma T_a^3}\Delta \end{aligned} \tag{12}$$

which has a dynamic that is also regulated by air vapor pressure deficit, and

$$\begin{aligned} E_T \quad &= C_E L_c \frac{\xi}{p}\left(\frac{2Cf(L_c) + 2L_c\epsilon\sigma T_a^3}{2Cf(L_c) + b\lambda C_E L_c \frac{\xi}{p}\Delta + 2L_c\epsilon\sigma T_a^3}\delta_a + \right. \\ &\left. \frac{R^A - L_c S_{nk} - 2L_c\epsilon\sigma T_a^4}{2Cf(L_c) + b\lambda C_E L_c \frac{\xi}{p}\Delta + 2L_c\epsilon\sigma T_a^3}\Delta\right) \end{aligned} \tag{13}$$

Equation (13) can be considered a generalisation of the Penman-Monteith equation (Brutsaert 1982). As such E_T, the solution of a system of equations, as well as solutions for the leaf temperature (from the temperature gap), the air humidity (from the pressure gap) and the sensible heat transport out (or into) the canopy are obtained. The independent variables are, besides radiation, the vapor pressure deficit of air, δ_a, and those variables so far hidden in C and C_E. Due to turbulent transport, both C and C_E certainly depend on the mean wind velocity, $\bar{u}$, but other dependencies can be present. In particular, if C or C_E depends on the leaves temperature the linearisation process would be complicated and other terms would appear in the solutions, as discussed in the next section. To establish a connection with the traditional approach, the PM formula can be derived from Equation (13) by setting $f(L_C) = 1$, $b = 1$, the factor "2" to 1, $C_E = C$, and removing the radiative response of leaves. The solution in Equation (13) depends solely on the air temperature T_a and does not consider the leaf temperature. However, as indicated in Equation (10), it is incorrect to interpret this as implying that the leaf temperature and air temperature are equal.

3 | The Expression of Conductances and the Consistency of Previous Derivations

In Equation (2), it is crucial to consider the conductance of the transpiring surface, taking into account the entire pathway of water within SPAC, which is typically conceptualised as consisting of five compartments: soil, roots, stem, leaves and air. In this simplified representation, it is believed that the flux follows a similar law as expressed in Equation (2) throughout the system, albeit with varying conductances (Nobel 1991; Taiz and Zeiger 2014). By assuming that no water mass accumulates within these compartments, it can be easily demonstrated that the overall flux of the system, spanning from soil to atmosphere, can be described using a law of the same form as Equation (2) where the total equivalent conductance is determined by taking the inverse of the sum of the inverses of the individual conductances. This concept exhibits a strict resemblance to the principles of electric circuitry (Bonan et al. 2021) and is commonly referred to as the resistance model of transpiration. Introducing water accumulation capacities would be more realistic but would render the mathematical problem not explicitly solvable. Therefore, the C_E in the transport law of Equation (2) is now understood to be:

$$C_E = \left(l_{sr}K_s^{-1} + g_{roots}^{-1} + g_{stem}^{-1} + g_s^{-1} + C_{air}^{-1}\right)^{-1} \tag{14}$$

where the conductance in soil is given by the hydraulic conductivity divided by a characteristic length of the soil-root interaction, $C_{soil} = K_s/l_{sr}$, and, in accordance with the literature, we have named the conductance of the leaves g_s. The conductance of the stem, g_{stem}, can be represented as a function of the comprehensive hydraulic conductivity K of the stem, given by $g_{stem} = K/l$, where l denotes the average length of flow paths through the xylem to the leaves. C_{air} can be determined using simplified assumptions, as described in Brutsaert (2023).

For simplicity, in the following discussion, we will focus on the conductance of the leaves as it is the primary site of resistance (i.e., the inverse of conductivity) (Soriano et al. 2020). Additionally, we will examine its relationship with stem conductivity.

The ultimate form of g_s depends on the concurrent processes of transpiration and photosynthesis, or the water supply and carbon assimilation, A_n, which is sustained for a wide range of temperatures, typically ranging from 0°C to 50°C (Bernacchi et al. 2009; Gabriel 2021). Photosynthesis also depends on other environmental factors, such as the amount of incident light, the water potential in the soil, the water pressure deficit and the CO_2 concentration (Lhomme 2001), and therefore, it is obvious to think that C_E depends on all of these factors. Of primary importance for our derivations, however, is that g_s depends upon temperature (Gabriel 2021). Generally, optimal temperatures for gross photosynthesis fall within the range of 15°C–40°C.

To account for these environmental effects, in the literature, there are two main families of parameterisations of the conductance of leaves (stomata conductance) g_s (Damour et al. 2010). The Jarvis parameterisation (Jarvis, Monteith, and Weatherley 1976) expresses g_s as a product of factors, which are dependent on environmental quantities such as photosynthetically active radiation, PAR, temperature, T, vapor pressure deficit, δ_a, leaf water potential ψ_l, and C_a, CO_2 concentration in air. The form of Jarvis' g_s is simply the result of complete expression of the influence of all the variables without any synergistic interactions:

$$g_s = \underbrace{g_{s,max} \cdot f_R(PAR) f_T(T_l) f_\delta(\delta_a) f_C(C_a)}_{g_{eff}} f_\psi(\psi_l) \tag{15}$$

where $g_{s,max}$ is the maximum conductance, without any kind of stress and in well-watered conditions (m s^{-1}), $f_R(PAR), f_T(T_l), f_\delta(\delta_a), f_\psi(\psi_l)$ and $f_C(C_a)$ are appropriate empirical functions with codomain in [0,1]. For purposes of our subsequent analysis, all the terms except for the one containing the dependence on ψ_l are grouped in g_{eff}. Other formulations (Damour et al. 2010; Allen 1986) can also contain further dependencies. The stress function for each influencing factor has various forms in the literature as reported for instance in Wang et al. (2016) and Liu et al. (2019) and Wang et al. (2020). However, the form of the function for the temperature appearing in Equation (15) is a bell–Gaussian–parabolic type of curve:

$$f_T(T_l) = b_3 \frac{T_l - T_{low}}{(T_{up} - T_l)^{b_4}} \tag{16}$$

where $b_3 = 1/(T_0 - T_{low})(T_{up} - T_0)^{b_4}$ and $b_4 = (T_{up} - T_0)/(T_h - T_{low})$. $f_T(T_l)$ is a dimensionless conductance varying between 1 at T_0 and zero at T_{low} and T_{up}, the lower and higher leaf temperature at which the curve meets the abscissa.

The forms of other stress factors in Equation (15) are presented in Appendix C.

The second type of parameterisation for g_s is due to the Ball–Berry–Leuning (BBL) (Ball, Woodrow, and Berry 1987; Leuning 1990; Dewar 2002), and it has been modified in various

ways since the original paper. For instance, in Dewar (2002), the form given to it is as follows:

$$g_B = g_0 + g_1 \frac{A_n}{(C_s - \Gamma)\left(1 + \frac{\delta_a}{e_0}\right)} \tag{17}$$

where Γ is the CO_2 concentration at the compensation point, that is, at which the rate of photosynthesis equates the rate of respiration; g_B is the Ball–Berry–Leuning conductance; g_0 is the value of g_B at the compensation point, and g_1 and e_0 are empirical coefficients; A_n is the net leaf CO_2 assimilation rate and either is a time-varying measured variable or requires the modelling of the carbon cycle; C_s is the CO_2 concentration at the leaf surface; and finally, δ_a is the water vapor pressure deficit. An interesting form of the BBL was obtained in Medlyn et al. (2011), under the hypothesis of optimal photosynthesis theory, which is as follows:

$$g_B = 1.6\left(1 + \frac{g_1}{\sqrt{\delta_a}}\right)\frac{A_n}{C_s} \tag{18}$$

where all the symbols have been explained before. Interestingly, Lin et al. (2015) provide values for the g_1 variable for various types of vegetation in different locations, as reported in Table C1 of Appendix C.

In the above BBL formulas, it is usually assumed that A_n can be approximated by a downward parabola, dependent on T_l, typically represented as follows:

$$A_n(T_l) = A_{\max} - b(T_l - T_{\text{opt}})^2 \tag{19}$$

In Equation (19), A_n represents the photosynthetic rate of carbon assimilation measured at leaf temperature T_l, $A_{\max}$ denotes the rate at the optimum temperature T_{opt} and the parameter b controls the sharpness of the parabolic curve. Also, in this treatment, the dependence on environmental factors is present, even if not usually explicated. For example, the three parameters of Equation (19) exhibit dependencies from the CO_2 content as justified in Yamaguchi et al. (2019), light saturation, as in Woods and Turner (1971), and are relatively resilient to direct water content, as in Cornic and Massacci (1996). Undoubtedly, achieving a consistent utilisation of the Ball–Berry–Leuning formula would necessitate the complete integration of the water budget and carbon budget, although this aspect is beyond the scope of the present paper.

Therefore, the formulation of the temperature stress in Equation (16) embeds a similar temperature dependence as in Equation (19), and similarly violates the hypotheses under which the solutions of the previous Section 2 was derived . The problem can be circumvented by taking the Taylor expansion of the C_E at first order, around the air temperature. Thus, Equation (2) can be rewritten as follows:

$$\begin{aligned} E_T &= (C_E(\delta_a, T_a, PAR, \theta) + C'_E(\delta_a, T_a, PAR, \theta,)\Delta T_\Delta) L_c \frac{\xi}{p}(\delta_a + \Delta T_\Delta) \\ &\approx C_E(\delta_a, T_a, PAR, \theta,) L_c \frac{\xi}{p}\delta_a + \\ &(C_E(\delta_a, T_a, PAR, \theta) L_c \frac{\xi}{p} + \underbrace{C'_E(\delta_a, T_a, PAR, \theta,) L_c \frac{\xi}{p}\delta_a)}_{\text{additional term}} \Delta T_\Delta \end{aligned} \tag{20}$$

which introduces an additional term in the denominator for the solution for T_Δ in Equation (10), thus producing the solution:

$$T_{\Delta_2} = \frac{R^A - b\lambda L_c C_E \frac{\xi}{p}\delta_a - L_c S_{nk} - 2L_c \epsilon\sigma T_a^4}{2Cf(L_c) + b\lambda C_E L_c \frac{\xi}{p}\Delta + 2L_c\epsilon\sigma T_a^3 + C'_E(\delta_a, T_a, PAR, \theta) L_c \frac{\xi}{p}\delta_a)\Delta} \tag{21}$$

Thus, accounting for the temperature dependence of conductance directly results in variations in leaf temperature. The additional term can be positive for temperatures below optimal temperature and negative for temperatures above it (Wang et al. 2020). Once substituted into Equations (3), (8) and (5), the above T_Δ changes the solutions for E_T, H, e_Δ. Notably, a term at the denominator dependent on δ_a is now present in Equation (21), which complicates the dependence on the water pressure deficit and could have some relevance under conditions of global warming where δ_a is foreseen to increase (Xu et al. 2024). Because of its form, the additional term C'_E brings a negative contribution for $T < T_{opt}$ and a positive contribution for $T > T_{opt}$.

In many implementations, such as in Bottazzi (2020), $f_T(T_l)$ is often substituted with $f'_T(T_a)$, which directly depends on air temperature. However, as seen in comparison with Equation (20), this assumption cannot be made approximately equivalent to the original formulation, even by redefining certain parameters related to xylem water potential, and this substitution can potentially introduce biases in the transpiration estimations.

The relative effect of stomatal conductance on T_Δ can be quantified by the ratio of Equation (21) over Equation (10):

$$T_{R_1} = \frac{2Cf(L_c) + b\lambda C_E L_c \frac{\xi}{p}\Delta + 2L_c\epsilon\sigma T_a^3}{2Cf(L_c) + b\lambda C_E L_c \frac{\xi}{p}\Delta + 2L_c\epsilon\sigma T_a^3 + C'_E(\delta_a, T_a, PAR, \theta) L_c \frac{\xi}{p}\delta_a)\Delta} \tag{22}$$

In the conductance formulas, another important factor is the conductance, C, associated with thermal energy exchange. Similar to C_{air}, this conductance is influenced by turbulent transport. The estimation of C typically assumes a similarity between the vegetated landscape and the airflow over a rough plane, where the air velocity may exhibit a logarithmic profile. Under these assumptions, Liu et al. (2007) provide a comprehensive review of various resistance expressions that can also be applied in this context. The same formulas, with appropriate parameter modifications, can also be used for C_{air} in Equation (14).

4 | Concepts and Equations of Water-limited Transpiration

The issue addressed in this section is how to effectively couple energy and water balances to estimate plant water use under stress conditions. This water-limited scenario, which respects water budget constraints, can be represented by recognising that plants sense water availability through water potential (Binks et al. 2024) and by incorporating a model of plant hydraulics. To begin, we can apply the Clausius–Clapeyron equation, accounting for the water-deficit-induced depression in the leaves due to

the Kelvin effect (Vesala et al. 2017; Bohren and Albrecht 1998). It reads as follows:

$$e^{\#}(T) = e^{*}(T_{ref})\exp\left[-\frac{\lambda m_{H_2O}}{R}\left(\frac{1}{T}-\frac{1}{T_{ref}}\right)\right]\exp\left(\frac{\psi_l V_{H_2O}}{RT}\right) \quad (23)$$

where $e^{*}(T_{ref}) = 0.611$ (Pa) is the saturation water vapor pressure at $T_{ref} = 273.15$ (K), a reference temperature; ψ_l is the (negative) water potential in leaves (Pa); V_{H_2O} is the molar volume of water (18×10^{-6} m^3 mol^{-1}); $\lambda = 2.2610^6$ (J kg^{-1}) is the enthalpy (latent heat) of vaporisation of water; R is the universal gas constant, equal to 8.31446 (J K $^{-1}$ mol^{-1}); $m_{H_2O} = 18{,}0152\,10^{-3}$ (kg mol^{-1}) is the molar mass of water; and T is the temperature (K).

The water budget was implicitly introduced in partial form in Section 3 when we formulated the Jarvis parameterisation of the conductances. In that context, we introduced the term $f_\psi(\psi_l)$, primarily on an empirical basis, to account for variations in the E_T flux in response to changes in leaf water potential ψ_l, which is itself dependent on soil and xylem water content. The rationale for including this term becomes clearer when considering the need to incorporate a simplified model of plant hydraulics, as explained below. The introduction of the new variable ψ_l in Equation (23) necessitates, in fact, adding another equation to the system described in Section 2 in order to balance the number of unknowns and equations. This equation is the water budget of the plant which we write and discuss below.

To keep the problem as simple as possible, it is assumed that the SPAC can be split into two functional parts, one including the soil and the stem (and where, with some loss of accuracy, roots are treated as the stem), SP_1, and the leaves with their stomata and the atmosphere, P_2A. SP_1 is treated as a single equivalent pipe, and the resulting water flux (sap flow) is eventually equalled to the transpiration out of the stomata. The resulting coupling of the water and the energy budgets can therefore be represented as in Figure 2 where S is the water storage in the plant, J_v is the water inputs from the stem and E_T is the transpiration in mass units. In Figure 2, the bridges, that is, the dashed lines ending with small empty squares, connect the same variables that are present in both the water and energy budgets after the appropriate transformation; thus, the graphic representation highlights all the relevant connections between the energy budget, the water budget and other variables that, at present, must be determined externally to the system of equations to be solved. After these choices and as shown in the figure, the water budget can be expressed by a simple equality:

$$J_v = E_T \quad (24)$$

where J_v is the sapflow and E_T is the transpiration.

This approach overlooks time lags that have been observed in plant response during sap-flow experiments (Kume et al. 2008; Ferraz et al. 2015), as well as phenomena such as water storage, discharge and refilling (Phillips et al. 2009; Oliva Carrasco et al. 2015; Wang et al. 2019). These factors can be thought as responsible for the resilience of plants to water stress and should be considered in a more refined approach but would render the mathematical problem not explicitly solvable.

We discuss the terms in Equation (24) separately. It is assumed that the flow in the roots and stems (sap flow) through the xylem occurs under laminar conditions and J_v can be estimated as follows (McDowell et al. 2008; Lin et al. 2015):

$$J_v = g_{SP_1}(\psi_x, \psi_s)\left(\psi_s - \psi_l\right) := g_{SP_1}(\psi_x, \psi_s)\psi_\Delta \quad (25)$$

where the effect of the gravitational potential has been neglected for simplicity and J_v is the flow that feeds transpiration rate; $g_{SP_1}(\psi_x, \psi_s)$ is a generalised form of the hydraulic conductance of SP_1, dependent on the average suction inside the xylem, ψ_x, and the soil, ψ_s. For the sake of simplicity, in this study the ψ_x is assumed either to be known or that it can be approximated by a simple function of ψ_l. $g_{SP_1}((\psi_x, \psi_s))$ can be expressed as follows:

$$g_{SP_1}(\psi_x, \psi_s) \approx \left[\frac{l_{sr}}{K_s(\psi_s)\Omega_s\rho_w} + \frac{l}{k_{max}K_x(\psi_x)\Omega_x}\right]^{-1} \quad (26)$$

where l_{sr} - is a characteristic length of the soil-roots interaction; Ω_s (m^2) is the surface through which the flux of water moves from the soil to roots (usually expressed as $\Omega_s = R_L V_R$ where R_L is the roots length (m m^{-3}) for unit soil volume and V_R (m^3) is the root volume); ρ_w (kg m^{-3}) is the water density; l (m) is the stem length, k_{max} is the maximum value possible of specific sap flow (kg m^{-2} s^{-1} Pa^{-1}) and Ω_x (m^2) is the cross-sectional area. Both K_s and $k_{max}K_x$ are hydraulic conductivities but expressed in different units, as customary of hydrology (the root term) and plant physiology (the xylem term) and clarified in the Supporting Information.

The xylem conductivity decreases when xylem becomes progressively embolised under increasing tension, proportionally to the distribution of occluded pathways (Venturas, Sperry, and Hacke 2017). Water stress induces embolism, freezing-thawing, and pathogens cause embolism but no one of the causes is related to stomatal functions (Tyree and Sperry 1989). The relationship between relative hydraulic conductivity and stem tension, which follows a sigmoidal form, see Appendix D, is well-documented in the literature (Venturas, Sperry, and Hacke 2017; Lehnebach et al. 2018).

As demonstrated in Manzoni, Vico, Katul, et al. (2013), Equation (25) exhibits a behaviour illustrated by the continuous grey curve in Figure 3, which displays a maximum value E_T as function of ψ_x, depending on the physical structure of the plant. This happens because g_{SP_1} is an increasing function of ψ_x, while the driving force, $(\psi_s - \psi_l) \approx -\psi_l$, is a decreasing function. However, g_{SP_1} is also a function of ψ_s and when the soil dries, the grey curves lowers to the brown curves of Figure 3.

Therefore, when $\psi_x \to -\infty$, the water flux to the leaves is limited by increasing embolism (Sperry, Stiller, and Hacke 2003; Venturas, Sperry, and Hacke 2017) without any action being necessary from the stomata. On the other hand, the stomatal behaviour, as reflected by g_s, is influenced by a set of feedback

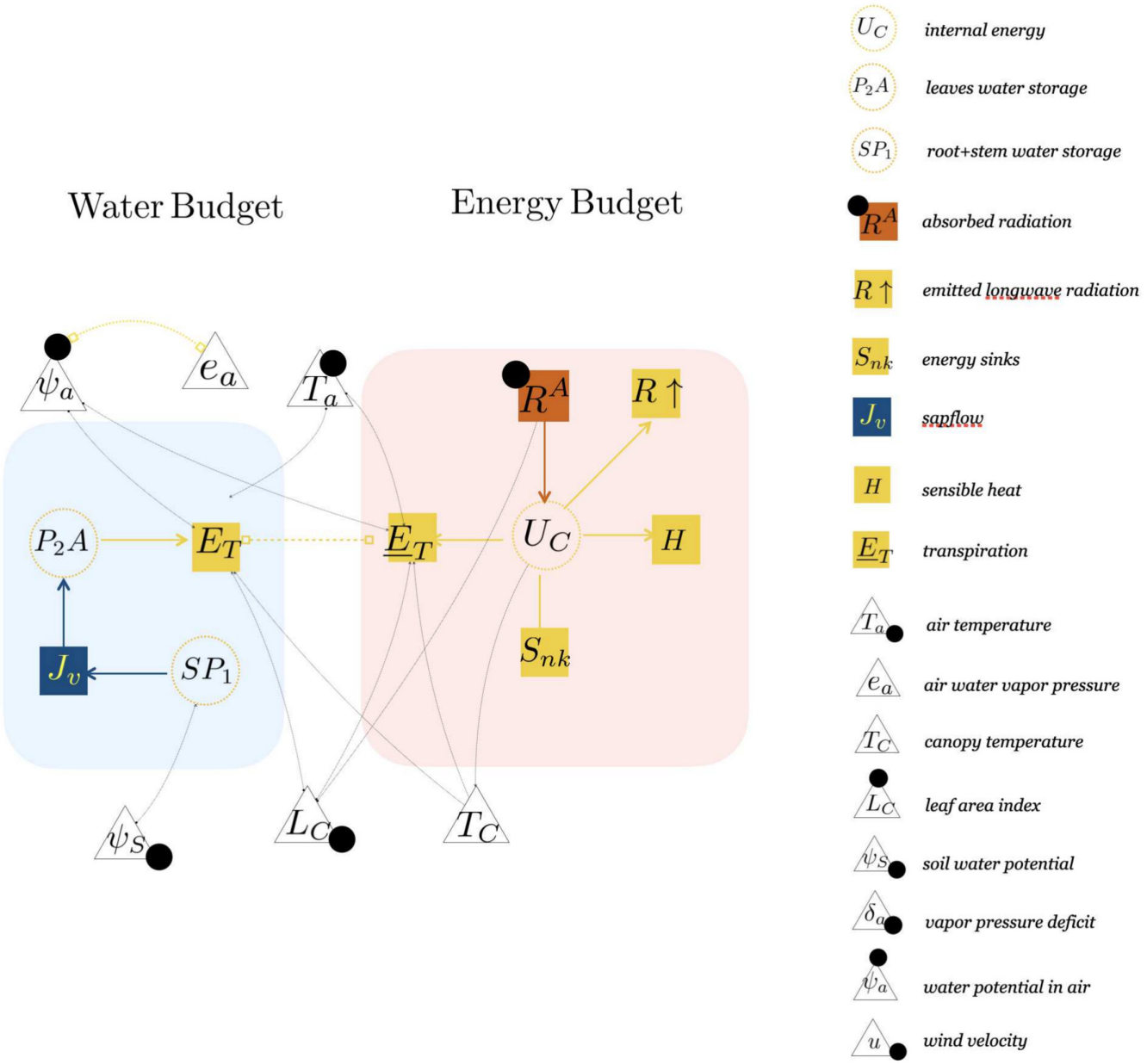

FIGURE 2 | The figure represents the combined water and energy budgets, and their interactions at plant scale. The red area of the EPN diagram is effectively the energy budget seen in Figure 1, while the blue area of the diagram represents the water budget. The water budget is influenced by two boundary conditions: the water potential in the soil (ψ_S) and the water potential in the air (ψ_a), which is related to the water vapor pressure through the Clausius–Clapeyron equation (e_a). Two compartments of the SPAC are distinguished: the soil-root-xylem (SP_1) and the leaves to air (P_2A). The flux between these two storages is represented by J_v, which denotes sap flow, while E_T represents transpiration from leaves to atmosphere. Transpiration appears in both the water and energy budgets, with the latter considering the transferred water mass multiplied by the latent heat of vaporisation for water. The red area, encompassing the energy budget, the internal energy of the plant system (U_C) was already described accurately in the caption of Figure 1 and it is not repeated here.

mechanisms associated with the plant's biochemical and water status (Taiz and Zeiger 2014; Buckley 2019). The role of the potential control of the stomata on the E_T can be understood when equating the sap flow to evapotranspiration, that is, substituting into Equations (24), (2) and (25), by posing the following:

$$\underbrace{g_{SP_1}(\psi_x,\psi_s)\psi_\Delta}_{J_v} = g_{P_2A}(\psi_x,\psi_s)L_c\frac{\xi}{p}(e_l-e_a) := \underbrace{g_{P_2A}(\psi_x,\psi_s)L_c\frac{\xi}{p}e_\Delta}_{E_T} \tag{27}$$

where

$$g_{P_2A} := [g_s^{-1}+C_{air}^{-1}]^{-1} \tag{28}$$

Because $e_l = e_l(\psi_l, T_l)$, that is, is estimated by means of Equation (23), it is also a function of ψ_l and not only of T_l, as in Equation (1).

It is important to note that the conceptual meaning of Equation (27) is not always fully explored in the existing literature. Not only can a plant system be viewed as a pipe with

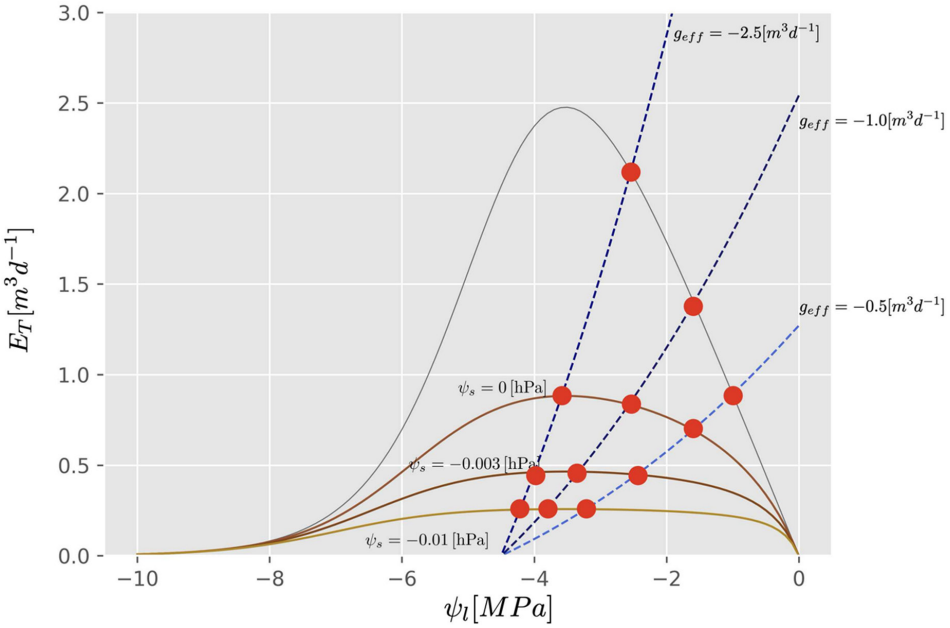

FIGURE 3 | The figure illustrates the working point of a plant, depicting the relationship between leaves' water potential (abscissa) and daily transpiration (ordinate). The grey line represents the optimal curve obtained using hydraulic conductivity as described in Kröber, Heklau, and Bruelheide (2015), while the xylem/leaves behaviour is estimated based on the approach outlined in Manzoni, Vico, Katul, et al. (2013). The stomatal conductance is determined according to Daly, Porporato, and Rodriguez-Iturbe (2004a) for three different values of $g_{s,max}$. Realistic values were selected, as explained in the Supporting Information, although certain crucial parameters such as the cross-sectional area of the tree or root density had to be assumed. The soil, assumed to be a silt loam, was characterised by estimating its conductivity using the Van–Genuchten Mualem parameterisation. The brownish curves indicate the limitations on transpiration due to decreasing soil pressure. Despite these limitations, the curve clearly demonstrates that when the plant xylem behaviour is coupled with soil behaviour, the transpiration rate is significantly constrained (as reported also in Carminati and Javaux 2020). The plant's working point, indicated by red dots, is determined by the intersection of the brownish curves with the dashed bluish curves representing stomatal behaviour as a function of xylem pressure. Each bluish curve corresponds to a hypothetical value of g_{eff} whose definition is in Equation (15).

distinct resistances (or conductances) that combine to form an overall resistance, but the appropriate continuity relationships must also be satisfied pairwise in adjacent plant and soil components, and especially between soil and roots, stem and leaves and leaves and air. As a result, the actual resistances (conductances) and water potential need to be carefully adjusted pairwise to ensure coherence, as clearly stated also in Manzoni, Vico, Katul, et al. (2013) and Manzoni, Vico, Porporato, and Katul (2013). However, typically, parameterisations of hydraulic conductivity in soil and stems and stomatal conductance are presented independently without ensuring their consistency.

The basic principles of hydraulics indicate that when the stomata are closed and the transpiration rate (E_T) is zero, there is no water flow from the soil and the leaf water potential (ψ_l) equals the soil water potential (ψ_s). When stomata open the transpiration dynamic is constrained on the brown curves in Equation (3) and ideally tends to gain the maximum rate (Manzoni, Vico, Katul, 2013). However, because this rate is quickly drying the soil, the optimal evaporation level and related photosynthetic activity are decreasing itself moving down from one brown curve to a lower one. Isohydric plants react by closing stomata to maintain the highest possible photosynthetic activity coherent with the water supply, and ultimately preventing the disruption of water flow and the plant's demise. The current understanding suggests that this happens through a complex set of feedback mechanisms (Eamus and Shanahan 2002; Buckley 2019; Sperry, Stiller, and Hacke 2003) that exploit a safety-efficiency trade-off that obviously differs between plant species and, up to a point, between individuals (Manzoni, Vico, Katul, et al. 2013; Manzoni, Vico, Porporato, and Katul, 2013). Building on the discussion above, it is evident that the role of stomata is not simply to "decrease" E_T but to "regulate" E_T in alignment with a plant's functional strategy and the surrounding environmental conditions. This process can be described as follows: when soil moisture diminishes, plants experience stem embolism, which reduces their transpiration and carbon gain rate and triggers stomatal closure to prevent further dehydration while maintaining a certain level of photosynthetic activity.

Figure 3 presents a comparison between the shape of the left-hand side of Equation (27), depicted by the brown curves, and the right-hand side, represented using a simplified parameterisation of the variable g_s as a function of ψ_l proposed by Daly, Porporato, and Rodriguez-Iturbe (2004b). The figure considers hypothetical variations of g_{eff} and is illustrated by blue dotted curves. The intersection of the brown and dotted curves determines the operating point of the plant, visually represented as a red point. The dotted curves are represented by varying value of g_{eff}, as defined in Equation (15) to account for the influence of the other environmental stresses that change during the day and through the seasons, thus determining different values of g_{eff}.

The overall result when there is an increase in evaporative demand from the atmosphere is that the increase in evaporation is less than linear (Sperry, Stiller, and Hacke 2003).

Another implication of the above analysis is that the water potential in plants is not solely attributed to the presence of micro or nano structures in leaves (as would be expected from an equilibrium interpretation based on capillarity, as claimed in physiology textbooks, e.g., Taiz and Zeiger 2014) but is primarily determined by the dynamics of water flow whose qualitative solution has just been illustrated.

One other important aspect of the aforementioned Figure 3 is that at ordinary soil suctions, the sap flow curves are quite flat and the working points return a quite constant sap flow with varying xylem/leaves pressure.

5 | Penman-Type Solutions for the Water-Limited Transpiration Case

To obtain the dynamics of transpiration from equations, we can pursue the same strategy that we adopted in Section 2 but linearising Equation (23) around the potential of the soil matrix, ψ_l, besides the air temperature, T_a. Arguably, such a linearisation could introduce errors, but we are more interested here in assessing the functional dependencies between variables rather than in obtaining accurate numbers. Therefore, the aim is to transform all equations, including the new Equation (27), into functions of the temperature gap, T_Δ, whose final expression is obtained by solving the energy budget. This implies expressing the water potential gap, ψ_Δ, as a function of T_Δ too. The details of the calculations are presented in Appendix E.

Accordingly, Equation (23) can be approximated in the form:

$$e_l(T_l, \psi_l) \sim \frac{\xi}{p}\hat{e} + \Delta_T T_\Delta + \Delta_\psi \psi_\Delta \tag{29}$$

with $\hat{e} := e(T_a, \psi_s)$ and

$$\Delta_T := \frac{1}{RT^2} e_l(T_l, \psi_l)\left(\lambda m_{H_2O} + \|\psi_l\| V_{H_2O}\right)_{T=T_a, \psi=\psi_s} \tag{30}$$

where it should be recalled that ψ_l is negative and, therefore, the term in brackets is always positive. Furthermore,

$$\Delta_\psi = \frac{V_{H_2O}}{RT} e^*(T)\Big|_{T=T_a, \psi=\psi_s} \tag{31}$$

Substituting the various terms in the energy budget, as in the previous sections, results in the following:

$$T_\Delta = \frac{R_a - \hat{C}_E L_c \frac{\xi}{p}(1 + \Delta_\psi A \hat{C}_E)\delta_a - 2\epsilon\sigma L_c T_a^4 - L_c S_{nk}}{C + \hat{C}_E L_c \frac{\xi}{p}(\Delta_T + B) + 2\epsilon\sigma L_c T_a^3} \tag{32}$$

where A and B are complex functions of Δ_ψ and Δ_T fully derived in Appendix E and contain the effects of water stress. This expression is certainly more complicated than Equation (10), but it is of the same type, and after substituting the temperature gap Equation (32) in Equations (3), (29) and (E11), we obtain the water-budget-aware thermal energy transport, transpiration and pressure gap. Their complete expressions are presented in Appendix E.

The equations derived from Equation (32) represent a further generalisation of the PM equation that includes the water budget and, to the best of our knowledge, has not been written or discussed before. The importance of water stress can be quantified by evaluating the ratio between Equations (32) and (21).

6 | The Sun–Shade Model

The conventional big-leaf approach, though widely used, is often regarded as inadequate for capturing the complexity of the energy budget (de Pury and Farquhar 1997). Therefore, in this section, we propose an extension toward a more realistic model, aiming to clarify which additional assumptions are necessary for improved accuracy. In detailed treatments of the SPAC, the amount of sunlight that each leaf receives depends on the position of the leaf within the canopy, the angle of the sun and the orientation of the leaf itself. Multilayered models of canopies (Goudriaan 1977; Baldocchi and Harley 1995) account for various factors such as leaf angle distribution, leaf density, leaf area index and the angle and intensity of the sun for a detailed computation of the light that reaches each leaf and the amount of light that is absorbed, transmitted or reflected.

A good compromise between the complicate multilayer models and the big-leaf approaches is dividing the canopy into two distinct conceptual layers: the sunlit layer and the shaded layer (Bonan et al. 2021). The sunlit layer represents the layer of the canopy where the leaves receive direct sunlight, while the shaded layer receives indirect or diffuse sunlight. It is important to note that these layers are conceptual in nature, as illustrated in Figure 4 and explained in detail in Appendix B.

Incoming radiation must be partitioned into two components to account for the distinct energy budgets of the sun-lit and shaded leaves, as depicted in the energy balance diagram in Figure 4. Consequently, sun-lit and shaded leaves have different temperatures T_{Sun} and T_{sh}, introducing an additional variable compared to big-leaf treatments. The equilibrium values of water vapor pressure in the sun and the shade, e^*_{sun} and e^*_{sh}, are also distinct variables, but their values can be derived by applying the Clausius–Clapeyron equation twice.

While Figure 4 shows that the only feedback usually implemented between the two canopy layers are the radiative exchanges, R_{SSh} (yellow) and R_{ShS} (orange) other exchanges of energy due to thermal energy transport could also occur. They depend, according to Stefan–Boltzman, on the fourth power of the leaves' temperature and by a partition coefficient that establishes which portion of the emitted radiation hits the other layer. For instance, including feedback with the terrain radiation is a straightforward extension that can be incorporated by adding a third layer hit by the residual radiation but is neglected in the present treatment for sake of simplicity.

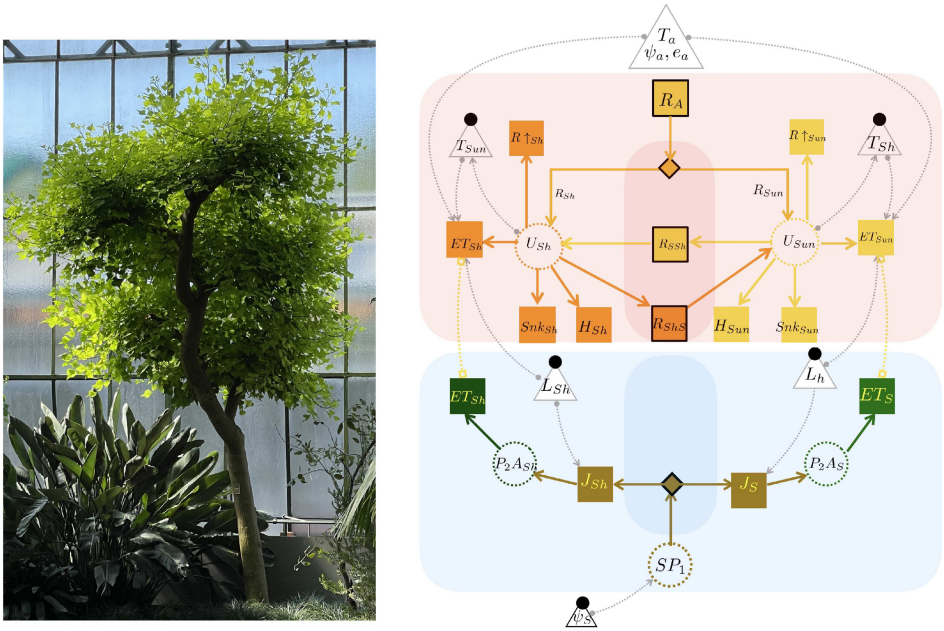

FIGURE 4 | The photo on the left side of the figure illustrates the rationale behind the Sun–Shade model. The lighter leaves are those directly hit by sunlight, while darker leaves are illuminated only by reflected and scattered light. Although not strictly categorised as sunlit and shaded layers, the distinction between the two sets of leaves in this case is quite evident. In most cases, the differentiation between the two sets may be less pronounced but still justifiable. This partition leads to a doubling of the elements in the combined water and energy budgets, and the EPN graph shown here directly highlights some key points of the partition at the centre of the figure and made more visible by the black frames. One notable aspect is the need to introduce a partition factor to divide the sap flow between shadowed leaves and sunlit leaves which needs to be addressed with some assumption. Additionally, the radiation input must be appropriately divided, as described in Appendix B. In the sun–shade modeling, longwave radiation exchanges between the two leaf compartments, that is, R_{SSh} and R_{ShS}, are also present and couple the two subsistems. The names used in the EPN graph follow the same nomenclature as in the previous figures, with updated subscripts: *Sh* for shaded leaves and *Sun* for sunlit leaves.

To translate into equations what is represented in Figure 4, on the top right side of Figure 4, is represented the sunlit canopy budget:

$$R_{Sun} + R_{ShS} - R_{SSh} = H_{sun} + b\lambda E_{T,Sun} + L_{Sun} S_{nk} \tag{33}$$

where R_{Sun} is the radiation received by the sunlit leaves and L_{Sun} is the leaf area index of the sunlit canopy; R_{ShS} is the radiative emission of the shaded leaves towards the sunlit leaves, and R_{SSh} is the radiative emission of the sunlit leaves towards the shaded ones.

The second budget, on the top left side of Figure 4, refers to the shaded canopy:

$$R_{Sh} - R_{ShS} + R_{SSh} = H_{Sh} + b\lambda E_{T,Sh} + L_{Sh} S_{nk} \tag{34}$$

where R_{Sh} is the radiation received by the shade leaves and L_{Sh} is the leaf area index of the canopy in the shade. The two energy budgets must be resolved simultaneously because of the feedback terms between them, which force an equalisation of leaves temperature via the exchange of longwave radiation. As in Section 4, the two energy budgets can be solved either without the water budget to obtain the energy limited solutions or coupled to the water budget to obtain the energy and water limited solutions. The bottom part of Figure 4 shows the companion water budgets for the shade leaves (left bottom) and the sunlit leaves (right bottom). Equation (27) is no longer valid alone and should be substituted with two separate equations:

$$C_J(\psi_x, \psi_s)\psi_{\Delta_j} = C_{E_j} \frac{\xi}{p} L_j e_{\Delta_j} \tag{35}$$

where $j \in \{Sun, Sh\}$ and where the total sap flow K_{max} is subdivided as in Kennedy et al. (2019), assigning to each compartment a flow proportional to the respective leaf area index, that is to say, $C_j = CL_j/L_c$.

The latter hypothesis assumes that the pathways from roots to leaves mix up the flows, and thus, we can attribute the same conductivity values to the xylems that feed sunlit and shaded leaves (Lehnebach et al. 2018). Therefore, the scheme applied in deriving the big-leaf equations for water and energy budgets can be replicated, as detailed in Appendix E. Eventually, for the sunlit leaves temperature gap, we have the following:

$$T_{\Delta_S} = \frac{R_S - \widehat{C}_E L_S \xi p^{-1}\left(1 + \Delta_{\psi_S} A_S \widehat{C}_E\right)\delta a - 2\epsilon\sigma L_S T a^4 - L_S S_{nk_S} + 2\alpha_{Sh}\epsilon L_{Sh}\sigma T_{Sh}^4}{C + \widehat{C}_E L_S \xi p^{-1}\left(\Delta_{T_S} + B_S\right) + 2\epsilon\sigma L_S T_a^3} \tag{36}$$

where the only variable previously unexplained is the term α_{Sh} (-) which is the portion of longwave radiation emitted by the shaded leaves towards the sunlit leaves. And for the shaded leaves:

$$T_{\Delta_{Sh}} = \frac{R_{Sh} - \widehat{C}_E L_{Sh} \xi p^{-1}\left(1 + \Delta_{\psi_{Sh}} A_{Sh} \widehat{C}_E\right)\delta a - 2\epsilon\sigma L_{Sh} T a^4 - L_{Sh} S_{nk_{Sh}} + 2\alpha_S \epsilon L_S \sigma T_S^4}{C + \widehat{C}_E L_{Sh} \xi p^{-1}\left(\Delta_{T_{Sh}} + B_{Sh}\right) + 2\epsilon\sigma L_{Sh} T_a^3} \tag{37}$$

where the term α_S (-) which is the portion of longwave radiation emitted by the sunlit leaves towards the shaded leaves. Equations (36) and (37) closely resemble Equation (32), each distinguished by its respective input term. The equations presented

above are not yet the solutions because Equation (36), and consequently T_{Δ_s}, depends on T_{Sh}, which in turn depends on $T_{\Delta_{Sh}}$, creating a mutual dependence between the two equations. Both temperature equations are quartic polynomials and they can be simultaneously solved using appropriate formulas or numerical methods for approximation. A key result of this derivation is also that the coupled water and energy budget of the sun–shade model can be solved explicitly, providing the temperature gaps, only upon the clarification of the mechanism of partitioning the water flux between the leaf layers. Further comments can be found in Section 7.

7 | Discussion

The procedures outlined in the previous sections are undoubtedly approximations and idealisations, which is a common and necessary practice in scientific modeling. Models are inherently simplifications of reality, designed to emphasise key elements while omitting complexities that are not immediately essential. This approach is particularly relevant in land surface modeling, where systems are highly complex, and researchers must balance accuracy with practical feasibility in their simulations and predictions. In this context, our work builds upon Penman's framework.

In pursuing our generalisations, we were guided by the principle of introducing only the minimum number of governing variables required, while maintaining a system of equations that could be solved explicitly. Although the literature on the PM formula spans 70 years and despite the simplifications required to derive it, hundreds of researchers have successfully used it to fit data. This has been possible for the ability of parameterisations to compensate for biases and uncertainties and, maybe, due to certain imprecision in the measures that should falsify the formula. We can also hypothesise that plants possess physiological mechanisms to maintain homeostasis around certain favourable conditions (Dewar 2002; Buckley 2005), which may not heavily depend on the specific details of hydraulic processes and may be readily described through suitably calibrated parameters. However, the investigation of how this happens is beyond the scope of this paper.

Our approach does not aim to produce a better fit to the available data but to theoretically refine and better define the scope of parameters, particularly the parameterisations of water conductance. Compared to the original PM formula, a straightforward generalisation involves introducing the canopy through the leaf area index variable. Although it is not easily measurable, extensive literature documents efforts in this area (e.g., Chen et al. 1997; Fang and Liang 2008; Zheng and Moskal 2009) indicating that it is a viable way to integrate canopies into modeling. One remaining area for exploration is determining the function $f(L_c)$ in Equation (3), which globally characterises how the sensible heat H couples with the atmosphere. This aspect cannot be separated from the analysis of the conductances C and C_{air}, to which it is conceptually linked. Numerous studies on leaf-to-atmosphere coupling have been conducted by micrometeorologists, with comprehensive reviews available in Bonan (2019), which can be a further reading to understand how these functions might be improved and with what level of accuracy.

This paper also brings evidence that the simplification made in the classical derivation of the PM formula, such as treating the aerodynamic conductance for sensible heat transport (C) and plant-to-atmosphere conductance (C_E) as equal, is probably an oversimplification. This equality is only valid, in our mathematics, if all plant-related conductances, like stomatal conductance (g_s), root conductance (g_{roots}) and stem conductance (g_{stem}), are very large, leaving the leaf-to-air conductance C_{air} in Equation (14) as the primary control over fluxes.

We also analysed the role of leaf temperature in conductance, as discussed in Section 3, suggesting a need for a correction term in deriving the temperature gap (i.e., in Equation 21). Although this term might ultimately be negligible, its potential influence warrants future investigation.

If models parameterise g_s using air temperature instead of leaf temperature, they risk introducing a significant bias, since this difference, established in Equation (10), is never negligible and has often been overlooked in traditional treatments of the PM equation.

As a result of the derivations in Sections 4 and 5, the integration of water availability into the SPAC dynamics is realised through three mechanisms. The first, often neglected, involves the generalisation of the Clausius–Clapeyron equation to include leaf water potential. The second aspect becomes significant when considering xylem hydraulics, that is, Equations (25) and (26), we need incorporating plant architecture and structure through appropriate traits. The third mechanism involves the action of stomata and its parameterisation, and it is the only considered for in the most basic PM formula.

With regard to the first mechanism, it could be argued that under normal conditions, the correction of the Clausius–Clapeyron relationship is minor. However, during drought conditions, this correction has been reported to reduce fluxes by about 15% (Vesala et al. 2017), suggesting that its inclusion could improve consistency in modeling plant physiology and better assess conductances. However, even if we neglect it, stem dimensions influence fluxes through variations in sap flow. In fact, Equation (25) underscores the need to evaluate both root and stem hydraulic conductivities, dependent on factors such as embolism levels and sap flow area, which are influenced by the size of tree and its branches (Tyree and Ewers 1991).

These geometric aspects are often overlooked in hydrological modeling but are well-recognised in plant physiology through concepts like leaf-specific conductivity (the hydraulic conductivity of a stem section divided by the leaf area distal to it) and the Huber value (sapwood cross-section divided by leaf area distal to the stem) (Soriano et al. 2020).

Researchers such as Manzoni, Vico, Katul, et al. (2013) and Manzoni, Vico,Porporato, and Katul (2013) have highlighted these factors as critical in determining overall stem conductances, but it is evident that accurate modeling requires relying on allometric relations between plant geometries and sapwood area (Anfodillo et al. 2016; Berry et al. 2018; Lehnebach et al. 2018). Given these considerations, the traditional formulation

of g_s might need rethinking or reparameterisation, as it was developed without accounting for these additional factors. In simplified approaches that neglect plant hydraulics, g_s certainly acts as a comprehensive parameter that serves as a surrogate for the missing elements.

Our model emphasises a stationary water budget rather than a modified Richards equation, and it could be a reasonable approximation when plant water capacity remains relatively stable. However, the literature suggests (Tyree and Ewers 1991; Binks et al. 2024) that this assumption may be unrealistic, potentially overlooking aspects that contribute to plant resilience during drought conditions. Incorporating plant capacitance (Bonan 2019) would change the set of governing variables, introducing the need for pressure-volume curves that relate plant water content to xylem water potential (Binks et al. 2024), analogous to soil-water retention curves. This addition would convert our algebraic equations into differential equations, requiring specialised numerical methods for solution.

Finally, the sun–shade model, described in Section 6, requires assumptions about water flux partitioning from soil to different radiation layers, and about the longwave radiation exchanges as highlighted in Figure 4. We assume that the distribution of water among leaves is uniform, although this may not always be the case. Further insights from plant physiology studies are required to refine the water and energy partitioning laws (Lehnebach et al. 2018). For future improvements, we recognise that certain assumptions in our approach, such as the use of a nonstationary energy budget, the exclusion of plant hydraulic capacitance (Meinzer et al. 2009), could be refined to enhance model accuracy without introducing excessive complexity. Additionally, incorporating the Richards equation for soil water dynamics, as proposed by Tubini and Rigon (2022), and using a little more complicate scheme of turbulent transport, as the one proposed in Poggi et al. (2004), could further improve model realism.

8 | Conclusions

This paper emphasises the essential role of adhering to mass and energy conservation principles in modeling plant transpiration. Its main achievements can be summarised as follows.

- It revisits the mathematical foundations of transpiration, addressing aspects that are often overlooked yet critical in traditional derivations.
- By reanalysing the big-leaf approach, we emphasise the significance of considering the leaf area index's influence on transpiration dynamics and the necessity for an appropriate treatment of radiation.
- Our derivation of the PM formula within the context of coupled equations highlights that, alongside transpiration E_T, key components such as sensible heat flux, H, pressure gradients, e_Δ, and temperature gap between air and leaves T_Δ can be derived. This temperature gap is an intrinsic feature of the PM model and its generalisations.
- The water potential, as derived here, emerges primarily from water dynamics rather than the capillarity of leaves, as traditionally emphasised in some literature.
- By isolating the nonstomatal factors, such as the thermodynamics of water vapor and the xylem's hydraulic limitations, this work singles out the role of stomatal regulation to its specific. Precisely, our results support the view that stomata primarily maintain hydraulic continuity under high transpiration demand, rather than directly reducing water loss, thus reversing the conventional causal narrative found in many textbooks.
- The derivation process allows us to identify the specific areas where information derived from plant allometry is crucial, particularly in the context of coupling sap flow with transpiration processes at the stem–leaf–atmosphere boundaries.
- One detail concerns stress models, where temperature dependence poses a challenge to the technical derivation of Penman equation. We propose that a correction in the temperature gap term can reconcile this discrepancy.
- By extending our analysis to the sunlit-sunshade model, we demonstrate that the progressive methodology adopted here applies to more realistic multilayer canopy structures with the use of water and radiation partition assumptions. However, the assumption of uniform water partitioning across the canopy layers warrants further experimental validation, as it may have significant implications for understanding plant physiological function.
- For field researchers, our method of explicitly solving water and energy budgets emphasises the practical importance of measuring the temperature gap between leaves and air. This gap can be directly incorporated into our intermediate equations, offering a valuable tool for comparing and refining different transpiration models.

While our mathematical framework has yet to be implemented in a computational model, we believe it provides a clear pathway for future model development. The advancements presented in this paper offer new opportunities to enhance the precision and depth of mechanistic ecohydrological research, addressing existing limitations and laying the foundation for further exploration. Furthermore, clarifying the fundamental mechanistic relationships, we believe that the paper has shed light on how and where mathematically, the complex interactions between physics, allometry and physiology align to produce plant responses that are simpler than their individual components suggest when examined in isolation.

Acknowledgements

The authors would like to thank Ing. Daniela Dal Monech for her comments to the manuscript and Joseph Tomasi for his invaluable revision of the language. This paper has been supported by MIUR Project (PRIN 2020) "Unravelling interactions between WATER 380 and carbon cycles during drought and their impact on water resources and forest and grassland ecosySTEMs in the Mediterranean climate (WATERSTEM) " (protocol code: 20202WF53Z) and "WAFER" @CNR projects (Consiglio Nazionale delle Ricerche). Open access publishing facilitated

by Universita degli Studi di Trento, as part of the Wiley - CRUI-CARE agreement.

Data Availability Statement

Data sharing is not applicable; no new data generated, or the article describes entirely theoretical research.

References

Abera, W., G. Formetta, M. Borga, et al. 2017. "Estimating the Water Budget Components and Their Variability in a Pre-Alpine Basin With JGrass-NewAGE." *Advances in Water Resources* 104: 37–54. https://doi.org/10.1016/j.advwatres.2017.03.010.

Abera, W., G. Formetta, L. Brocca, et al. 2017. "Modeling the Water Budget of the Upper Blue Nile Basin Using the JGrass-NewAge Model System and Satellite Data." *Hydrology and Earth System Sciences* 21, no. 6: 3145–3165. https://doi.org/10.5194/hess-21-3145-2017.

Allen, R. G. 1986. "A Penman for All Seasons." *Journal of Irrigation and Drainage Engineering* 112, no. 4: 348–368. https://doi.org/10.1061/(ASCE)0733-9437(1986)112:4(348).

Anfodillo, T., G. Petit, F. Sterck, et al. 2016. "Allometric Trajectories and Stress: A Quantitative Approach." *Frontiers in Plant Science* 7: 1866.

Baldocchi, D. D., and P. C. Harley. 1995. "Scaling Carbon Dioxide and Water Vapour Exchange From Leaf to Canopy in a Deciduous Forest. II. Model Testing and Application." *Plant, Cell & Environment* 18, no. 10: 1157–1173. https://doi.org/10.1111/j.1365-3040.1995.tb00626.x.

Ball, J. T., I. E. Woodrow, and J. A. Berry. 1987. "A Model Predicting Stomatal Conductance and its Contribution to the Control of Photosynthesis Under Different Environmental Conditions." In *Progress in Photosynthesis Research*, edited by J. Biggins, Vol. 62, 221–224. Springer Netherlands.

Bancheri, M., F. Serafin, and R. Rigon. 2019. "The Representation of Hydrological Dynamical Systems Using Extended Petri Nets (EPN)." *Water Resources Research*. https://doi.org/10.1029/2019WR025099.

Banerjee, T., F. De Roo, and M. Mauder. 2017. "Explaining the Convector Effect in Canopy Turbulence by Means of Large-Eddy Simulation." *Hydrology and Earth System Sciences* 21, no. 6: 2987–3000. https://doi.org/10.5194/hess-21-2987-2017.

Bernacchi, C. J., D. M. Rosenthal, C. Pimentel, et al. 2009. "Modeling the Temperature Dependence of C3 Photosynthesis." In *Photosynthesis In Silico*, 231–246. Springer Netherlands.

Berry, Z. C., N. Looker, F. Holwerda, et al. 2018. "Why Size Matters: The Interactive Influences of Tree Diameter Distribution and Sap Flow Parameters on Upscaled Transpiration." *Tree Physiology* 38, no. 2: 263–275.

Binks, O., A. Konings, P. Meir, et al. 2024. "A Theoretical Framework to Quantify Ecosystem Pressure- Volume Relationships." *Global Change Biology*.

Bohren, C. F., and B. A. Albrecht. 1998. *Atmospheric Thermodynamics*. Oxford University Press.

Bonan, G. 2019. *Climate Change and Terrestrial Ecosystem Modeling*. Cambridge University Press. https://doi.org/10.1017/9781107339217.

Bonan, G. B., E. G. Patton, J. J. Finnigan, and others. 2021. "Moving Beyond the Incorrect But Useful Paradigm: Reevaluating Big-Leaf and Multilayer Plant Canopies to Model Biosphere-Atmosphere Fluxes–A Review." *Agricultural and Forest*. https://doi.org/10.1016/j.agrformet.2021.108435.

Bottazzi, M. 2020. "Transpiration Theory and the Prospero Component of GEOFrame." Ph.D. Thesis, University of Trento.

Brutsaert, W. 1982. *Evaporation Into the Atmosphere*. Kluver Academics. https://doi.org/10.1007/978-94-017-1497-6.

Brutsaert, W. 2023. *Hydrology*. Cambridge University Press. https://doi.org/10.1017/9781316471562.

Buckley, T. N. 2005. "The Control of Stomata by Water Balance." *New Phytologist* 168, no. 2: 275–292.

Buckley, T. N. 2019. "How do stomata Respond to Water Status?." *New Phytologist* 224, no. 1: 21–36. https://doi.org/10.1111/nph.15899.

Carminati, A., and M. Javaux. 2020. "Soil Rather than Xylem Vulnerability Controls Stomatal Response to Drought." *Trends in Plant Science* 25, no. 9: 868–880. https://doi.org/10.1016/j.tplants.2020.04.003.

Cassini, A. 2021. "Deidealized Models." In *Models and Idealizations in Science: Artifactual and Fictional Approaches*, edited by A. Cassini and J. Redmond, 87–113. Springer International Publishing. https://doi.org/10.1007/978-3-030-65802-1.

Chen, J. M., P. M. Rich, S. T. Gower, et al. 1997. "Leaf Area Index of Boreal Forests: Theory, Techniques, and Measurements." *Journal of Geophysical Research* 102, no. D24: 29429–29443.

Cornic, G., and A. Massacci. 1996. "Leaf Photosynthesis Under Drought Stress." In *Photosynthesis and the Environment*, edited by N. R. Baker, 347–366. Springer Netherlands.

Corripio, J. G. 2003. "Vectorial Algebra Algorithms for Calculating Terrain Parameters from DEMs and Solar Radiation Modelling in Mountainous Terrain." *Geographic Information System* 17, no. 1: 1–23. https://doi.org/10.1080/713811744.

Cowan, I. R., and G. D. Farquhar. 1977. "Stomatal Function in Relation to Leaf Metabolism and Environment." *Symposia of the Society for Experimental Biology* 31: 471–505.

Daly, E., A. Porporato, and I. Rodriguez-Iturbe. 2004. "Coupled Dynamics of Photosynthesis, Transpiration, and Soil Water Balance. Part II: Stochastic Analysis and Ecohydrological Significance." *Journal of Hydrometeorolog* 5, no. 3: 559–566. https://doi.org/10.1175/1525-7541(2004)005<0546:CDOPTA>2.0.CO;2.

Daly, E., A. Porporato, and I. Rodriguez-Iturbe. 2004. "Coupled Dynamics of Photosynthesis, Transpiration, and Soil Water Balance. Part I: Upscaling From Hourly to Daily Level." *Journal of Hydrometeorolog* 5, no. 3: 546–558. https://doi.org/10.1175/1525-7541(2004)005<0546:CDOPTA>2.0.CO;2.

Damour, G., T. Simonneau, H. Cochard, et al. 2010. "An Overview of Models of Stomatal Conductance at the Leaf Level." *Plant, Cell & Environment* 33, no. 9: 1419–1438. https://doi.org/10.1111/j.1365-3040.2010.02181.x.

de Pury, D. G. G. 1995. "Scaling photosynthesis and Water Use From Leaves to Paddocks." Ph.D. Thesis, The Australian National University.

de Pury, D. G. G., and G. D. Farquhar. 1997. "Simple Scaling of Photosynthesis From Leaves to Canopies Without the Errors of Big-Leaf Models." *Plant, Cell & Environment* 20, no. 5: 537–557. https://doi.org/10.1111/j.1365-3040.1997.00094.x.

Deardorff, J. W. 1978. "Efficient Prediction of Ground Surface Temperature and Moisture, With Inclusion of a Layer of Vegetation." *Journal of Geophysical Research* 83, no. C4: 1889. https://doi.org/10.1029/JC083iC04p01889.

Dewar, R. C. 2002. "The Ball-Berry-Leuning and Tardieu-Davies Stomatal Models: Synthesis and Extension Within a Spatially Aggregated Picture of Guard Cell Function." *Plant, Cell & Environment* 25, no. 11: 1383–1398. https://doi.org/10.1046/j.1365-3040.2002.00909.x.

Dewar, R., A. Mauranen, A. Mäkelä, et al. 2018. "New Insights Into the Covariation of Stomatal, Mesophyll and Hydraulic Conductances From Optimization Models Incorporating Nonstomatal Limitations to Photosynthesis." *New Phytologist* 217, no. 2: 571–585. https://doi.org/10.1111/nph.14848.

Duursma, R., and B. Choat. 2017. "Fitplc - An R Package to Fit Hydraulic Vulnerability Curves." *Journal of Plant Hydraulics* 4: e002. https://doi.org/10.20870/jph.2017.e002.

Eagleson, P. S. 1978. "Climate, Soil, and Vegetation: 3. A Simplified Model of Soil Moisture Movement in the Liquid Phase." *Water Resources Research* 14, no. 5: 722–730. https://doi.org/10.1029/WR014i005p00722.

Eagleson, P. S. 2005. *Ecohydrology: Darwinian Expression of Vegetation Form and Function*. Cambridge University Press.

Eamus, D., and S. T. Shanahan. 2002. "A Rate Equation Model of Stomatal Responses to Vapour Pressure Deficit and Drought." *BMC Ecology* 2, no. 1: 8. https://doi.org/10.1186/1472-6785-2-8.

Fang, H., and S. Liang. 2008. "Leaf Area Index Models." In *Encyclopedia of Ecology*, 2139–2148. Elsevier.

Ferraz, T. M., A. T. Netto, F. De Oliveira Reis, et al. 2015. "Relationships Between Sap-Flow Measurements, Whole-Canopy Transpiration and Reference Evapotranspiration in Field-Grown Papaya (Carica Papaya l.)."*Theoretical and Experimental Plant Physiology* 27, no. 3: 251–262. https://doi.org/10.1007/s40626-015-0049-z.

Gabriel, C. 2021. "Effects of Temperature on Photosynthesis." Accessed: 2023-8-1.

Goudriaan, J. 1977. *Crop Micrometeorology: A Simulation Study*. Pudoc, Center for Agricultural Publishing and Documentation.

Hirose, T. 2004. "Development of the Monsi–Saeki Theory on Canopy Structure and Function." *Annals of Botany* 95, no. 3: 483–494. https://doi.org/10.1093/aob/mci047.

Jarvis, P. G., J. L. Monteith, and P. E. Weatherley. 1976. "The Interpretation of the Variations in Leaf Water Potential and Stomatal Conductance Found in Canopies in the Field." *Philosophical Transactions of the Royal Society B: Biological Sciences* 273, no. 927: 593–610. https://www.jstor.org/stable/2417554.

Joshi, J., B. D. Stocker, F. Hofhansl, et al. 2022. "Towards a Unified Theory of Plant Photosynthesis and Hydraulics." *Nature Plants* 2022: 1–13. https://doi.org/10.1038/s41477-022-01244-5.

Jovanovic, N., and S. Israel. 2012. "Critical Review of Methods for the Estimation of Actual Evapotranspiration in Hydrological Models." *Evapotranspiration-Remote Sensing and Modeling*: 24. https://www.intechopen.com/chapters/26111.

Katul, G. G., S. Palmroth, and R. Oren. 2009. "Leaf stomatal Responses to Vapour Pressure Deficit Under Current and CO(2)-Enriched Atmosphere Explained by the Economics of Gas Exchange." *Plant, Cell & Environment* 32, no. 8: 968–979. https://doi.org/10.1111/j.1365-3040.2009.01977.x.

Kennedy, D., S. Swenson, K. W. Oleson, et al. 2019. "Implementing Plant Hydraulics in the Community Land Model, Version 5." *Journal of Advances in Modeling Earth Systems* 11, no. 2: 485–513. https://doi.org/10.1029/2018MS001500.

Kröber, W., H. Heklau, and H. Bruelheide. 2015. "Leaf Morphology of 40 Evergreen and Deciduous Broadleaved Subtropical Tree Species and Relationships to Functional Ecophysiological Traits." *Plant Biology* 17, no. 2: 373–383. https://doi.org/10.1111/plb.12250.

Kume, T., H. Komatsu, K. Kuraji, et al. 2008. "Less Than 20-min Time Lags Between Transpiration and Stem Sap Flow in Emergent Trees in a Bornean Tropical Rainforest." *Agricultural and Forest Meteorology* 148, no. 6: 1181–1189. https://doi.org/10.1016/j.agrformet.2008.02.010.

Lawrence Dingman, S. 2015. *Physical Hydrology: Third Edition*. Waveland Press.

Lehnebach, R., R. Beyer, V. Letort, et al. 2018. "The Pipe Model Theory Half a Century on: A Review." *Annals of Botany* 121, no. 5: 773–795. https://doi.org/10.1093/aob/mcx194.

Leuning, R. 1990. "Modelling Stomatal Behaviour and Photosynthesis of Eucalyptus Grandis." *Functional Plant Biology* 17, no. 2: 159–175. https://doi.org/10.1071/PP9900159.

Lhomme, J.-P. 2001. "Stomatal Control of Transpiration: Examination of the Jarvis-Type Representation of Canopy Resistance in Relation to Humidity." *Water Resources Research* 37, no. 3: 689–699. https://doi.org/10.1029/2000WR900324.

Lin, Y.-S., B. E. Medlyn, R. A. Duursma, et al. 2015. "Optimal Stomatal Behaviour Around the World." *Nature Climate Change* 5, no. 5: 459–464. https://doi.org/10.1038/nclimate2550.

Liu, N., H. Wang, X. He, et al. 2019. "A Hybrid Transpiration Model for Water-Limited Conditions." *Journal of Hydrology* 578: 124104. https://doi.org/10.1016/j.jhydrol.2019.124104.

Liu, S., L. Lu, D. Mao, et al. 2007. "Evaluating Parameterizations of Aerodynamic Resistance to Heat Transfer Using Field Measurements." *Hydrology and Earth System Sciences* 11, no. 2: 769–783. https://doi.org/10.5194/hess-11-769-2007.

Macfarlane, C., D. A. White, and M. A. Adams. 2004. "The Apparent Feed-Forward Response to Vapour Pressure Deficit of Stomata in Droughted, Field-Grown Eucalyptus Globulus Labill." *Plant, Cell & Environment* 27, no. 10: 1268–1280. https://doi.org/10.1111/j.1365-3040.2004.01234.x.

Manzoni, S., G. Vico, G. Katul, et al. 2013. "Hydraulic Limits on Maximum Plant Transpiration and the Emergence of the Safety-Efficiency Trade-Off." *New Phytologist* 198, no. 1: 169–178. https://doi.org/10.1111/nph.12126.

Manzoni, S., G. Vico, A. Porporato, et al. 2013. "Biological Constraints on Water Transport in the Soil–Plant–Atmosphere System." *Advances in Water Resources* 51, no. C: 292–304. https://doi.org/10.1016/j.advwatres.2012.03.016.

Mauder, M., T. Foken, and J. Cuxart. 2020. "Surface-Energy-Balance Closure Over Land: A Review." *Boundary-Layer Meteorology* 177, no. 2: 395–426. https://doi.org/10.1007/s10546-020-00529-6.

McDowell, N., W. T. Pockman, C. D. Allen, et al. 2008. "Mechanisms of Plant Survival and Mortality During Drought: Why Do Some Plants Survive While Others Succumb to Drought?." *New Phytologist* 178, no. 4: 719–739. https://doi.org/10.1111/j.1469-8137.2008.02436.x.

Medlyn, B. E., R. A. Duursma, D. Eamus, et al. 2011. "Reconciling the Optimal and Empirical Approaches to Modelling Stomatal Conductance." *Global Change Biology* 17, no. 6: 2134–2144. https://doi.org/10.1111/j.1365-2486.2010.02375.x.

Meinzer, F. C., D. M. Johnson, B. Lachenbruch, et al. 2009. "Xylem Hydraulic Safety Margins in Woody Plants: Coordination of Stomatal Control of Xylem Tension With Hydraulic Capacitance." *Functional Ecology* 23, no. 5: 922–930.

Mencuccini, M., and J. Comstock. 1997. "Vulnerability to Cavitation in Populations of Two Desert Species, Hymenoclea Salsola and Ambrosia Dumosa, From Different Climatic Regions." *Journal of Experimental Botany* 48, no. 6: 1323–1334. https://doi.org/10.1093/jxb/48.6.1323.

Monsi, M., and T. Saeki. 1953. "The Light Factor in Plant Communities and Its Significance for Dry Matter Production." *Japanese Journal of Botany*.

Monson, R., and D. Baldocchi. 2014. *Terrestrial Biosphere-Atmosphere Fluxes*. Cambridge University Press. https://doi.org/10.1017/CBO9781139629218.

Monteith, J. L. 1981. "Evaporation and Surface Temperature." *Quarterly Journal of the Royal Meteorological Society* 107, no. 451: 1–27. https://doi.org/10.1002/qj.49710745102.

Muller, J. D., E. Rotenberg, F. Tatarinov, et al. 2021. "Evidence for Efficient Non-Evaporative Leaf-to-Air Heat Dissipation in a Pine Forest Under Drought Conditions." https://doi.org/10.1111/nph.17742.

Neufeld, H. S., D. A. Grantz, F. C. Meinzer, et al. 1992. "Genotypic Variability in Vulnerability of Leaf Xylem to Cavitation in Water-Stressed and Well-Irrigated Sugarcane." *Plant Physiology* 100, no. 2: 1020–1028. https://doi.org/10.1104/pp.100.2.1020.

Nobel, P. 1991. *Pysicochemical and Environmental Plant Physiology*. Academic Press, Inv.

Ogle, K., J. J. Barber, C. Willson, et al. 2009. "Hierarchical Statistical Modeling of Xylem Vulnerability to Cavitation." *New Phytologist* 182, no. 2: 541–554. https://doi.org/10.1111/j.1469-8137.2008.02760.x.

Oliva Carrasco, L., S. J. Bucci, D. Di Francescantonio, et al. 2015. "Water Storage Dynamics in the Main Stem of Subtropical Tree Species Differing in Wood Density, Growth Rate and Life History Traits." *Tree Physiology* 35, no. 4: 354–365. https://doi.org/10.1093/treephys/tpu087.

Pammenter, N. W., and C. Van der Willigen. 1998. "A Mathematical and Statistical Analysis of the Curves Illustrating Vulnerability of Xylem to Cavitation." *Tree Physiology* 18, no. 8-9: 589–593. https://doi.org/10.1093/treephys/18.8-9.589.

Penman, H. L., and B. A. Keen. 1948. "Natural Evaporation From Open Water, Bare Soil and Grass." *Proceedings of the Royal Society of London. Series A - Mathematical and Physical Sciences* 193, no. 1032: 120–145. https://doi.org/10.1098/rspa.1948.0037.

Phillips, N. G., F. G. Scholz, S. J. Bucci, et al. 2009. "Using Branch and Basal Trunk Sap Flow Measurements to Estimate Whole-Plant Water Capacitance: Comment on Burgess and Dawson (2008)." *Plant Soil* 315, no. 1: 315–324. https://doi.org/10.1007/s11104-008-9741-y.

Poggi, D., G. G. Katul, and J. D. Albertson. 2004. "A Note on the Contribution of Dispersive Fluxes to Momentum Transfer Within Canopies." *Boundary-Layer Meteorology* 111, no. 3: 615–621. https://doi.org/10.1023/B:BOUN.0000016563.76874.47.

Porporato, A., and J. Yin. 2022. *Ecohydrology: Dynamics of Life and Water in the Critical Zone*. Cambridge University Press.

Rawlings, J. O., and W. W. Cure. 1985. "The Weibull Function as a Dose-Response Model to Describe Ozone Effects on Crop Yields1." *Crop Science* 25, no. 5. https://doi.org/10.2135/cropsci1985.0011183X002500050020x.

Rodriguez-Iturbe, I. 2000. "Ecohydrology: A Hydrologic Perspective of Climate-Soil-Vegetation Dynamics." *Water Resources Research* 36, no. 1. https://doi.org/10.1029/1999WR900210.

Rodriguez-Iturbe, I., and A. Porporato. 2007. *Ecohydrology of Water-Controlled Ecosystems: Soil Moisture and Plant Dynamics*. Cambridge University Press. https://doi.org/10.1017/CBO9780511535727.

Ryu, Y., D. D. Baldocchi, H. Kobayashi, et al. 2011. "Integration of MODIS Land and Atmosphere Products With a Coupled-Process Model to Estimate Gross Primary Productivity and Evapotranspiration From 1 km to Global Scales." *Global Biogeochemical Cycles* 25, no. 4. https://doi.org/10.1029/2011GB004053.

Schymanski, S. J., and D. Or. 2017. "Leaf-Scale Experiments Reveal an Important Omission in the Penman–Monteith Equation." *Hydrology and Earth System Sciences* 21, no. 2: 685–706. https://doi.org/10.5194/hess-21-685-2017.

Soriano, D., A. Echeverria, T. Anfodillo, et al. 2020. "Hydraulic Traits Vary as the Result of Tip-to-Base Conduit Widening in Vascular Plants." *Journal of Experimental Botany* 71, no. 14: 4232–4242. https://doi.org/10.1093/jxb/eraa157.

Sperry, J. S., V. Stiller, and U. G. Hacke. 2003. "Xylem Hydraulics and the Soil–Plant–Atmosphere Continuum: Opportunities and Unresolved Issues." *Agronomy Journal* 95, no. 6: 1362–1370. https://doi.org/10.2134/agronj2003.1362.

Taiz, L., and E. Zeiger. 2014. *Plant Physiology and Development*. Sinauer.

Tubini, N., and R. Rigon. 2022. "Implementing the Water, HEat and Transport Model in GEOframe (WHETGEO-1D v.1.0): Algorithms, Informatics, Design Patterns, Open Science Features, and 1D Deployment." *Geoscientific Model Development* 15, no. 1: 75–104. https://doi.org/10.5194/gmd-15-75-2022.

Tyree, M. T., and F. W. Ewers. 1991. "The Hydraulic Architecture of Trees and Other Woody Plants." *New Phytologist* 119, no. 3: 345–360.

Tyree, M. T., and J. S. Sperry. 1989. "Vulnerability of Xylem to Cavitation and Embolism." *Annual Review of Plant Physiology and Plant Molecular Biology* 40, no. 1: 19–36. https://doi.org/10.1146/annurev.pp.40.060189.000315.

Venturas, M. D., J. S. Sperry, and U. G. Hacke. 2017. "Plant Xylem Hydraulics: What We Understand, Current Research, and Future Challenges." *Journal of Integrative Plant Biology* 59, no. 6: 356–389. https://doi.org/10.1111/jipb.12534.

Vesala, T., S. Sevanto, T. Grönholm, et al. 2017. "Effect of Leaf Water Potential on Internal Humidity and CO2 Dissolution: Reverse Transpiration and Improved Water Use Efficiency Under Negative Pressure." *Frontiers in Plant Science* 8: 54. https://doi.org/10.3389/fpls.2017.00054.

Wang, C., P. Yang, Y. Li, et al. 2013. "Characteristics of E. japonicus Stomatal Conductance Under Water-Deficit Stress Using a Nonlinear Jarvis Modified Model." *Mathematical and Computer Modelling* 58, no. 3: 799–806. https://doi.org/10.1016/j.mcm.2012.12.024.

Wang, H., H. Guan, N. Liu, et al. 2020. "Improving the Jarvis-Type Model With Modified Temperature and Radiation Functions for Sap Flow Simulations." *Journal of Hydrology* 587: 124981. https://doi.org/10.1016/j.jhydrol.2020.124981.

Wang, H., H. Guan, and C. T. Simmons. 2016. "Modeling the Environmental Controls on Tree Water Use at Different Temporal Scales." *Agricultural and Forest Meteorology* 225: 24–35. https://doi.org/10.1016/j.agrformet.2016.04.016.

Wang, H., I. C. Prentice, T. F. Keenan, et al. 2017. "Towards a Universal Model for Carbon Dioxide Uptake by Plants." *Nat Plants* 3, no. 9: 734–741. https://doi.org/10.1038/s41477-017-0006-8.

Wang, H., D. Tetzlaff, and C. Soulsby. 2019. "Hysteretic Response of Sap Flow in Scots Pine (Pinus sylvestris) to Meteorological Forcing in a Humid Low Energy Headwater Catchment." *Ecohydrology* 12, no. 6: e2125. https://doi.org/10.1002/eco.2125.

Wang, Y.-P., and R. Leuning. 1998. "A Two-Leaf Model for Canopy Conductance, Photosynthesis and Partitioning of Available Energy I:: Model Description and Comparison With a Multi-Layered Model." *Agricultural and Forest Meteorology* 91, no. 1: 89–111. https://doi.org/10.1016/S0168-1923(98)00061-6.

Werner, C., L. K. Meredith, S. N. Ladd, et al. 2021. "Ecosystem Fluxes During Drought and Recovery in an Experimental Forest." *Science* 374, no. 6574: 1514–1518.

Werner, C., U. Wallrabe, A. Christen, et al. 2024. "ECOSENSE - Multi-Scale Quantification and Modelling of Spatio-Temporal Dynamics of Ecosystem Processes by Smart Autonomous Sensor Networks." *Research Ideas and Outcomes* 10.

White, D. A., C. L. Beadle, P. J. Sands, et al. 1999. "Quantifying the Effect of Cumulative Water Stress on Stomatal Conductance of Eucalyptus globulus and Eucalyptus nitens: A Phenomenological Approach." *Australian Journal of Plant Physiology* 26, no. 1: 17–27. https://doi.org/10.1071/PP98023.

Woods, D. B., and N. C. Turner. 1971. "Stomatal Response to Changing Light by Four Tree Species of Varying Shade Tolerance." *New Phytologist* 70, no. 1: 77–84. https://doi.org/10.1111/j.1469-8137.1971.tb02512.x.

Xu, W., X. Xia, S. Piao, et al. 2024. "Weakened Increase in Global Near-Surface Water Vapor Pressure During the Last 20 Years." *Geophysical Research Letters* 51, no. 2.

Yamaguchi, D. P., D. Mishima, K. Nakamura, et al. 2019. "Limitation in the Photosynthetic Acclimation to High Temperature in Canopy Leaves of Quercus serrata." *Frontiers in Forests and Global Change* 2. https://doi.org/10.3389/ffgc.2019.00019.

Yu, L.-Y., H.-J. Cai, Z. Zheng, et al. 2017. "Towards a More Flexible Representation of Water Stress Effects in the Nonlinear Jarvis Model." *Journal of Integrative Agriculture* 16, no. 1: 210–220. https://doi.org/10.1016/S2095-3119(15)61307-7.

Zheng, G., and L. M. Moskal. 2009. "Retrieving Leaf Area Index (LAI) Using Remote Sensing: Theories, Methods and Sensors." *Sensors* 9, no. 4: 2719–2745.

Supporting Information

Additional supporting information can be found online in the Supporting Information section.

Appendix A

Table of Symbols

Appendix A includes most of the parameters and symbols used in this study. Table A1 includes symbols, their definitions and if available, their values.

Appendix B

On the Parameterization of Radiation as it Interacts With Canopies

A concise description of the incoming solar radiation reaching plants is an essential ingredient for any transpiration model. A treatment of radiation that is suitable for hydrological models without introducing unnecessary complexities can be found in Corripio (2003).

Assuming that $R{\downarrow}_s$ is the total downwelling, incoming, shortwave radiation and $R{\downarrow}_l$ is the total downwelling, longwave radiation, then

$$R_i{\downarrow} = R_i^A + R_i^R + R_i^T \tag{B1}$$

for $i \in \{s, l\}$ where the superscript A means absorbed, R is for reflected and T is for transmitted. Of the three components, only the absorbed radiation contributes to the energy budget of the canopy. Usually, it is posed that $R_i^R = \alpha R{\downarrow}_i$, where α is the albedo, while R_i^T is estimated through variations of the Lambert–Beer law, as described, for instance, in de Pury (1995), Chapter 6, Section 6.2.3.2.

The theory of how radiation impacts canopies goes back to Monsi and Saeki (1953) and is best summarized in Goudriaan (1977) and Hirose (2004). In the seminal papers, canopies are treated as an oriented continuums, the direction of which is given by the sun beam downward into the canopy. In this case, the cumulative amount of leaves going deeper and deeper into the canopy can serve as a coordinate with values that go from 0 at the top of the canopy to L_c, the total leaf area index (LAI), at the bottom of the canopy.

Even though very complex and detailed models of canopies can be envisioned, an often-used, idealised compromise is the sun–shade model, in which all the complexity of the canopy is reduced to two ideal layers: one layer of leaves that are directly sunlit and the other of leaves that are shaded. Besides, part of the radiation can pass through the canopy and hit the soil. As shown in Figure B1, the two layers really are more conceptual than geometrical, since in reality the set of sunlit leaves can be quite sparse and spread deep into the canopy, depending on leaf distribution and orientation.

The sun–shade model first estimates the penetrating solar beam (direct light) per unit ground area $R_b(L)$, which decreases in accordance with a Lambert–Beer type law (as taken from de Pury (1995), Chapter 6.2):

$$R_b(L) = R_b(0)e^{-k_b L\Omega} \tag{B2}$$

where $R_b(0)$ is the direct solar radiation on top of the canopy, k_b is a beam radiation extinction coefficient of canopy, function of the solar elevation angle and Ω is a correction factor, called the clumped canopy coefficient, that has been introduced in recent papers such as Ryu et al. (2011) to account for the distribution of leaves. This "sunfleck" contribution is represented in Figure B1 by the orange beams hitting and passing through part of the canopy.

The determination of the absorption of all light fluxes per unit leaf area is based on the alteration in radiation with depth, expressed mathematically as the first differential. The impact of leaf absorption is contingent upon whether scattering is integrated into the flux or treated as a distinct component. In cases where a flux excludes scattering, the absorbed light undergoes further reduction due to the absorptivity of the leaves, denoted as $(1 - \sigma_c)$, where σ_c represents the leaf scattering coefficient. Conversely, when the flux is a net flux that already encompasses canopy reflectance and scattering, the calculation of absorbed light is simply derived from the differential.

Considering only direct beam sunlight, the average beam sunlight absorbed per unit leaf area ($R'_{Sun}(L)$) is calculated by the first differential of Equation (B2) by the leaf absorptivity:

$$R'_b(L) = (1-\sigma_c)\Omega k_b R_b(0)e^{-k_b L\Omega} \tag{B3}$$

which represents the sunlight absorbed by a layer of leaves between the levels $[L_{AI}, L_{AI} + dL_{AI}]$.

The fraction of leaves in sunfleacks, f_{Sun}, is derived from the beam penetration function:

$$f_{Sun}(L) = e^{-k_b L\Omega} \tag{B4}$$

The radiation absorbed by the sunlit leaf fraction of the canopy $R_{Sun}(L_c)$ is calculated as the integral of the absorbed radiation over the L_c and the sunlit leaf area fraction:

$$R_{Sun}(L_c) = \int_0^{L_c} R'_b(L) f_{Sun}(L) dL = R_b(0)(1-\sigma_c)(1-e^{-k_b L_c \Omega}) \tag{B5}$$

Similar treatments to the one used to derive Equation (B5) are reserved for the scattered and diffuse light, represented in Figure B1 by the blue and dark yellow dashed lines. Unlike the direct beam, scattered light and diffuse light are thought to be isotropic from all directions. The details of the calculations can be found in Section 6.2 of de Pury (1995), with slightly different notation then that used here.

Although direct light and diffuse light are usually considered separately, the scattered light component is dealt with together with the other two, as in equations (2) to (11) in Ryu et al. (2011), ensuring that all the direct shortwave radiation, not only the photosynthetic active radiation (PAR), is included so that the energy budget is considered in its completeness. The leaves in shade are hit by scattered and diffuse light but also by the radiation reflected by the soil (Ryu et al. 2011). Finally, radiation is subdivided into its longwave and shortwave components, as is quantified in Equations (12) to (21) in Ryu et al. (2011). Overall, we have at least 10 different components of radiation. However, they still do not contain the radiative feedbacks, which are essential in stabilising leaf temperature. Any layer, because its temperature, emits a quantity of radiation:

$$R_{fj} = -2\epsilon\sigma T_i^4 \tag{B6}$$

where $j = \{sun, shade\}$ and $i = \{shade, sun\}$ and the same layer receives from the other layer an amount of radiation:

$$R_{fi} = \epsilon\sigma T_j^4 \tag{B7}$$

with the subscripts exchanged. Equation (B6) is thought equally likely to be shared between other parts of the canopy and the external environment. Therefore, each conceptual layer is receiving a radiation quantity from any other layer as in Equation (B7).

Finally, with a sun–shade model, the residual radiation hits the terrain and is partially reflected back, and, as mentioned before, this reflected that radiation is added back to the shaded compartment of the model.

Similar arguments, with a few modifications, can be used to treat the more complex case of the sun–shade model which is discussed briefly in Appendix E.

Appendix C

Stomatal Conductance Functions

While there are many stomatal conductance functions in literature that could be considered, here we present in more detail only two: the Jarvis parameterization (Jarvis, Monteith, and Weatherley 1976), especially

TABLE A1 | List of symbols used in this paper and their definition.

Symbols	Unit	Value	Definition
α_b	—	—	Albedo for direct solar radiation.
α_d	—	—	Albedo for diffuse radiation.
b	—	—	Parameter for epistomatous and amphystomatous leaves in Equation (5).
C	m s^{-1}	—	Heat transport conductance, derived as detailed in Brutsaert (1982) and Banerjee, De Roo, and Mauder (2017).
$\widehat{C}$	—	—	Dimensionless conductance derived from the analysis of turbulent behaviour in proximity to the leaves.
C_{air}	m s^{-1}	—	Air conductance, it can be determined using simplified assumptions, as described in Brutsaert (2023).
C_E	m s^{-1}	—	Transpiration conductance.
$\widehat{C}_E$	m s^{-1}	—	Transpiration conductance function of T_a and ψ_s.
c_p	J kg^{-1} K^{-1}	—	Thermal capacity of air.
Δ	—	—	Derivative of the Clausius–Clapeyron equation (1) estimated at air temperature T_a.
δ_a	Pa	—	Vapor pressure deficit: $(e_a^* - e_a)$
δ_l	Pa	—	Vapor pressure gap in leaves: $(e_l^* - e_l)$
e^*	Pa	—	Saturation vapor pressure at temperature T.
e_0^*	Pa	611	Saturation vapor pressure at the reference temperature T_0.
e_a	Pa	—	Water vapor pressure in the atmosphere.
e_a^*	Pa	—	Saturation vapor pressure in air.
e_Δ	Pa	—	Pressure gap between leaf and air, defined as $(e_l - e_a)$.
e_l	Pa	—	Water vapor pressure at the leaf surface.
$e^\#$	Pa	—	Modified water vapor tension in Equation (23).
ϵ	—	—	Emissivity of the canopy.
g_s	m s^{-1}	—	Conductance of the leaves.
$g_{P_2A}(\psi_x, \psi_s)$	—	—	Control parameter for stomatal conductance, dependent on average suction inside the xylem, ψ_x, and soil, ψ_s.
$g_{SP_1}(\psi_x, \psi_s)$	—	—	Generalised hydraulic conductance of SP_1, dependent on average suction inside the xylem, ψ_x, and soil, ψ_s.
H	W m^{-2}	—	Sensible heat.
H_{Sh}	W m^{-2}	—	Sensible heat of the shaded leaves.
H_{Sun}	W m^{-2}	—	Sensible heat of the sunlit leaves.
k'_b	—	—	Extinction factor for direct solar beam.
k'_d	—	—	Extinction factor for diffuse radiation.
k_{max}	kg m^{-1} s^{-1} Pa^{-1}	—	Maximum possible value of specific sap flow.
$K_s(\psi_s)$	—	—	Soil hydraulic conductivity, dependent on soil suction ψ_s.
$K_x(\psi_x)$	—	—	Xylem hydraulic conductivity, dependent on xylem suction ψ_x.
L_c	—	—	Leaf Area Index of the whole canopy.
L_{Sh}	—	—	Leaf area index of the canopy in the shade.
L_{Sun}	—	—	Leaf area index of the sunlit canopy.

(Continues)

TABLE A1 | (Continued)

Symbols	Unit	Value	Definition
l	m	—	Length of the stem.
l_{sr}	m	—	Characteristic length of the soil-roots interaction.
λ	J kg^{-1}	2.26×10^{6}	Latent heat of vaporization for water.
m_{H_2O}	kg mol^{-1}	18.01528	Molar mass of water.
$O(\Delta T_a^2)$	—	—	Terms of Taylor's expansion higher than 1.
Ω_s	m^2	—	Surface through which the flux of water moves from the soil to roots.
Ω_x	m^2	—	Cross-sectional area (CSA).
p	Pa	—	Atmospheric pressure.
R	J K^{-1} mol^{-1}	8.3144	Universal gas constant.
R^A	W m^{-2}	—	Radiation absorbed by the canopy.
$R_b(0)$	W m^{-2}	—	Direct sunlight at the top of the canopy.
$R_d(0)$	W m^{-2}	—	Diffuse sunlight at the top of the canopy.
$R\uparrow$	W m^{-2}	—	Radiation canopy emission.
R_L	m m^{-3}	—	Root length for unit soil volume.
R_{Sh}	W	—	Radiation received by the shaded leaves.
R_{ShS}	W	—	Radiative emission of the shaded leaves towards the sunlit leaves.
R_{SSh}	W	—	Radiative emission of the sunlit leaves towards the shaded ones.
R_{Sun}	W	—	Radiation received by the sunlit leaves.
ρ_a	kg m^{-3}	—	Air density.
ρ_w	kg m^{-3}	1000	Water Density.
S_{nk}	W m^{-2}	—	Energy Sink for the energy absorbed by photosynthetic processes.
σ	W m^{-2} K^{-4}	5.67×10^{-8}	Stefan-Boltzmann constant.
T	K	—	Absolute temperature.
T_a	K	—	Air temperature.
T_Δ	K	—	Temperature gap, defined as $(T_l - T_a)$.
T_l	K	—	Leaf temperature.
$T_0 = T_{ref}$	K	273.15	Reference temperature.
$\bar{u}$	m s^{-1}	—	Module of the mean horizontal wind velocity.
V_{H_2O}	m^3 mol^{-1}	18×10^{-6}	Molar volume of water.
V_R	m^3	—	Root volume.
ξ	—	0.622	Ratio between dry and wet air gas constants.
ψ_l	Pa	—	Negative water potential in leaves.
ψ_s	Pa	—	Soil suction.

Note: When applicable, also, their value is present.

the one proposed by White et al. (1999) and by Macfarlane, White, and Adams (2004) and a second interesting function proposed by Ball–Berry–Leuning (BBL) (Ball, Woodrow, and Berry 1987; Leuning 1990; Dewar 2002).

The Jarvis stress factor is a concept used in modeling the stomatal conductance of plants under different water stress conditions. It is based on the Jarvis model (Equation 15) which incorporates various environmental factors to estimate stomatal conductance. Several studies have explored the performance of different water stress indicators in the Jarvis model. Yu et al. (2017) compared three indicators: soil water content, J_S; leaf-air temperature difference, J_T; and leaf level water stress index ($CWSI_L$), J_C. They found that the J_T and J_C models had better simulation accuracy than the J_S model. Wang et al. (2013) developed an improved

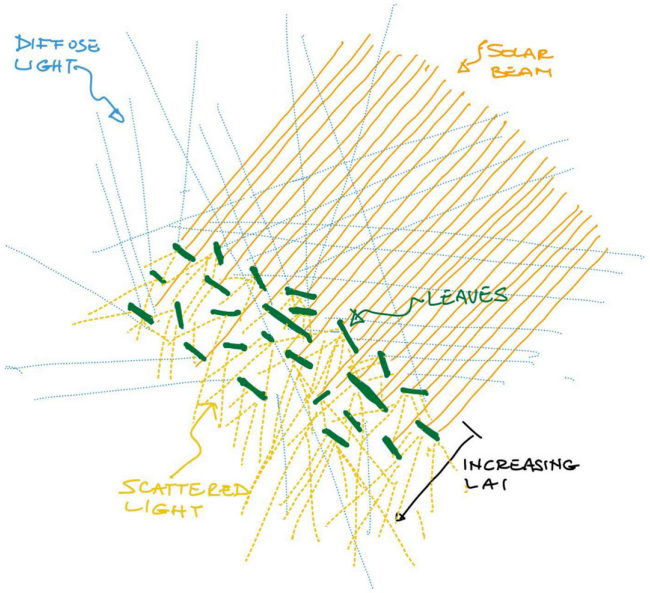

FIGURE B1 | Schematic representation of a portion of a canopy being struck by a solar beam. The canopy is represented by the set of green segments, the incoming sunlit is depicted in orange, the light scattered by the leaves in yellow and the diffuse atmospheric light in light blue.

Jarvis model and found that it had better simulation results compared to the original Jarvis model and an artificial neural network model. These studies highlight, firstly, the importance of considering environmental factors and using appropriate indicators in the Jarvis model to accurately estimate stomatal conductance under water stress conditions and secondly, the variety of studies that have been carried out on the Jarvis model.

Jarvis, Monteith, and Weatherley (1976) introduced some functions to parametrize the stress functions of the model. In literature, there are several types of conductance models; however, the environmental stress functions implemented in GEOET model (EvapoTranpiration model of GEOframe), and especially in the `geoet.stressfactor` package, follow the version of the model proposed by White et al. (1999) and by Macfarlane, White, and Adams (2004), where the conductance is equal to the following:

$$g_s = g_{s,max} \cdot f(R_{PAR}) \cdot f_T(T_a) \cdot f(VPD) \cdot f(\psi_l) \tag{C1}$$

where $g_{s,max}$ is the conductance without any kind of stress and in well-watered conditions (m s^{-1}), while $f(R_{PAR}), f_T(T_a), f(VPD)$ and $f(\psi_l)$ are the normalised stress factors, empirical functions with codomain in [0,1], induced, respectively, by the photosynthetically active radiation (PAR), the air temperature, the water pressure deficit and the leaf water potential. To simplify, one usually calculates $f(\psi_l)$ as a function of soil water content, denoted as $f(\theta)$.

- **Total solar radiation stress**

According to White et al. (1999), the solar radiation stress can be computed as follows:

$$f(R_{PAR}) = \left[\frac{1}{2\theta}\left(\alpha R_{sw} + 1 - \sqrt{(\alpha R_{sw}+1)^2 - 4\theta\alpha R_{sw}}\right)\right]^{-1} \tag{C2}$$

where α and θ are the slope and shape parameters of the stress function $f(R_{PAR})$ and are set equal to 0.005 and 0.85 (-), respectively. R_{sw} is the total solar radiation, expressed in μmol $m^{-2}s^{-1}$. If we want to express it in W m^{-2}, we must include a conversion factor equal to $\approx \frac{1}{4.6}$.

TABLE C1 | Estimates of g_1 by different classification schemes according to Lin et al. (2015).

Classification scheme	Class	g_1 mean	g_1 SE
a_Pathway	C4	1.62	0.03
	C3	4.16	0.01
b_Plantform	Gymno. tree	2.35	0.02
	shrub	3.32	0.05
	Angio. tree	3.97	0.02
	Grass	5.25	0.13
	Savanna tree	5.76	0.22
	Crop	5.79	0.04
c_T region	Artic	2.22	0.07
	Boreal	2.19	0.02
	Temperate	4.31	0.02
	Tropical	4.43	0.08
d_W Region	$MI < 0.5$	3.77	0.03
	$0.5 \leq MI < 1$	4.69	0.04
	$1.0 \leq MI < 1.5$	3.87	0.03
	$MI > 1.5$	4.02	0.02
e_PFTs	C4 grass	1.62	0.03
	Ever.gymno.tree	2.35	0.02
	Deci.savanna. tree	2.98	0.39
	Shrub	3.32	0.05
	Ever. angio. tree	3.37	0.03
	Trop. Rainforest tree	3.77	0.04
	Deci. angio. tree	4.64	0.04
	C3 grass	5.25	0.13
	C3 crop	5.79	0.04
	Ever. savanna tree	7.18	0.25

- **Air temperature stress**

Following Jarvis, Monteith, and Weatherley (1976) and White et al. (1999), the air temperature stress factor can be computed as follows:

$$f_T(T_a) = b(T_a - T_l)(T_h T_a)^c \tag{C3}$$

where b and c are defined as follows:

$$c = \frac{T_h - T_0}{T_0 - Tl} \tag{C4}$$

$$b = \frac{1}{(T_0 - Tl)(T_h - T_0)^c} \tag{C5}$$

where T_0 is the temperature at maximum conductance (C) and T_l and T_h are the lower and upper temperatures of the range for which a positive stomatal conductance is predicted (C). White et al. (1999) assigned the values for T_l, T_0 and T_h equal to 0°C, 17°C and 38°C, respectively. These parameters can be set a priori or calibrated.

- **Vapour pressure deficit stress**

The vapor deficit stress factor can be estimated as in White et al. (1999):

$$f(VPD) = 1.1\exp(-0.63 \cdot VPD) \tag{C6}$$

where VPD is the vapour pressure deficit value and when $VPD = 0.2kPa$, $f(VPD) = 1$.

The second type of parameterization for stomatal conductance is due to Ball–Berry–Leuning (BBL) (Ball, Woodrow, and Berry 1987; Leuning 1990; Dewar 2002), and it has been modified in various ways since the original paper. An interesting form of the BBL was obtained in Medlyn et al. (2011), under the hypothesis of optimal photosynthesis theory (Equation 18).

Lin et al. (2015) give values for the g_1 variable for various types of vegetation in different locations, reported in Table C1.

Appendix D

The Hydraulic Conductivity of Plants

To understand more about plant hydraulics, we recommend starting with Venturas, Sperry, and Hacke (2017) and Lehnebach et al. (2018), which is read as a complement. However, in this appendix, we concentrate on the decline of stem conductivity with stem suction.

Literature reports that it declines with stem potential according to a sigmoid form (an exceeding probability like s function), and various forms were used to parameterize this behaviour. In particular,

- the exponential-sigmoid (Pammenter and Van der Willigen 1998)

$$K(\psi) = K_{max}\left(1 - \frac{1}{1+\exp(a(\psi - b))}\right) \tag{D1}$$

where a and b are a scale parameter and location parameter, respectively.

- the Weibull (Rawlings and Cure 1985; Neufeld et al. 1992)

$$K(\psi) = K_{max}e^{-\left(\frac{\psi}{\alpha}\right)^{\beta}} \tag{D2}$$

where α is the water potential at which the hydraulic conductivity is reduced to $1/e$ of its maximum value and β is a shape parameter that determines the slope of the curve.

- the Gompertz (Mencuccini and Comstock 1997)

$$K(\psi) = 1 - ae^{-be^{-c\psi}} \tag{D3}$$

where b and c are the two parameters.

- the power law (Wang et al. 2017)

$$K(\psi) = \left(\frac{1}{2}\right)^{\left(\frac{\psi}{\psi 50}\right)^{b}} \tag{D4}$$

where ψ_{50} is the value of water potential at which 50% of the maximum conductivity is lost.

However, for historical reasons, in the literature on plant physiology, the decline of water conductivity is modelled using PLC curves, which represent the percent loss conductivity. PLC have a one-to-one relation with hydraulic conductivity that is given by the formula:

$$K(\psi) = K_{max}\left(1 - \frac{PLC(\psi)}{100}\right) \tag{D5}$$

Some researchers have found it useful to treat the parametrization of the previous curves differently. For instance, Ogle et al. (2009) prefer to express the loss of conductivity in the Weibul probability distribution function as a function of ψ_{50}, an indication that was taken in Duursma and Choat (2017) to implement their R software fitplc. The latter paper also tries to evaluate the error of estimation and the parameters that they reproduce in their Table 1 for some plant species, information that could be used as reference for typical estimations.

Appendix E

The Water Limited Case: Detailed Calculations

If we consider Equation (27), where we equated the sap flow to evapotranspiration, $J_v = E_T$, we can then obtain the following:

$$C(\psi_x, \psi_s)\psi_\Delta = C_E\frac{\xi}{p}\left(\hat{e} + \Delta_T T_\Delta + \Delta_\psi \psi_\Delta - e_a\right) = C_E\frac{\xi}{p}\left(\delta_a + \Delta_T T_\Delta + \Delta_\psi \psi_\Delta\right) \tag{E1}$$

where it has been assumed that $\hat{e} = e(\psi_s, T_a) \approx e(T_a)$, being the dependence of Equation (23) on ψ_s negligible for the normal range of its variation. Before moving further, however, we have to consider whether C_E depends on the independent variables T_Δ and ψ_Δ, as we did in Section 3.

A proper linearization of Equation (E1) requires the Taylor expansion of the conductance C_E:

$$C_E(T_l, \psi_l) \approx \hat{C}_E + C_\psi \psi_\Delta + C_T T_\Delta \tag{E2}$$

where $\hat{C}_E := C_E(T_a, \psi_s)$, C_ψ is the first order partial derivative of C_E with respect to ψ_l estimated in ψ_s and C_T is the first-order derivative with respect to T estimated in T_a.

Introducing this into the first-order Taylor expansion of the right-hand side of Equation (E1) results in the following:

$$\begin{aligned}&(\hat{C}_E + C_\psi \psi_\Delta + C_T T_\Delta)\frac{\xi}{p}(\delta_a + \Delta_T T_\Delta + \Delta_\psi \psi_\Delta) \approx \\ &\frac{\xi}{p}\left[\hat{C}_E(\delta_a + \Delta_T T_\Delta + \Delta_\psi \psi_\Delta) + \delta_a C_\psi \psi_\Delta + C_T \delta_a T_\Delta\right] = \\ &\frac{\xi}{p}\left(\hat{C}_E\delta_a + (\hat{C}_E\Delta_T + \delta_a C_T)T_\Delta + (\hat{C}_E\Delta_\psi + \delta_a C_\psi)\psi_\Delta\right)\end{aligned} \tag{E3}$$

Therefore,

$$C(\psi_x, \psi_s)\psi_\Delta = \frac{\xi}{p}\left(\hat{C}_E\delta_a + (\hat{C}_E\Delta_T + \delta_a C_T)T_\Delta + (\hat{C}_E\Delta_\psi + \delta_a C_\psi)\psi_\Delta\right) \tag{E4}$$

To keep the derivation simple, we will assume here that $\psi_x = \alpha\psi_l^{(t-1)}$, with ψ_x approximated as a fraction α of ψ_l estimated at time $t-1$. That is to say, we update $\psi_x(t)$, at time t, using ψ_x of the previous time step, $t-1$. This assumption seems justified by various empirical studies, such as Lehnebach et al. (2018), because the equilibration of the water potential of mesophyll cells and the xylem is rapid. Alternative simplifications can be considered, but we do not dig into them here to maintain the treatment simple and explicitly tractable.

The terms multiplying ψ_Δ can now be collected as follows:

$$\left[\frac{p}{\xi}C(\psi_x, \psi_s) - \hat{C}_E\Delta_\psi - \delta_a C_\psi\right]\psi_\Delta = \hat{C}_E\delta_a + (\hat{C}_E\Delta_T + \delta_a C_T)T_\Delta \tag{E5}$$

From which, we finally have the following:

$$\psi_\Delta = \frac{\widehat{C}_E \delta_a}{\frac{p}{\xi} C(\psi_x, \psi_s) - \widehat{C}_E \Delta_\psi - \delta_a C_\psi} + \frac{\widehat{C}_E \Delta_T + \delta_a C_T}{\frac{p}{\xi} C(\psi_x, \psi_s) - \widehat{C}_E \Delta_\psi - \delta_a C_\psi} T_\Delta \tag{E6}$$

or

$$\psi_\Delta = A \check{C}_E \delta_a + B T_\Delta \tag{E7}$$

with

$$A := \frac{1}{\frac{p}{\xi} C(\psi_x, \psi_s) - \widehat{C}_E \Delta_\psi - \delta_a C_\psi} \tag{E8}$$

and

$$B := \frac{\widehat{C}_E \Delta_T + \delta_a C_T}{\frac{p}{\xi} C(\psi_x, \psi_s) - \widehat{C}_E \Delta_\psi - \delta_a C_\psi} \tag{E9}$$

After this treatment, the approximated expression for e_l can be written as follows:

$$e_l(T_l, \psi_l) \approx \hat{e} + \Delta_T T_\Delta + \Delta_\psi (A \widehat{C}_E \delta_a + B T_\Delta) = \hat{e} + \Delta_\psi A \widehat{C}_E \delta_a + (\Delta_T + B) T_\Delta \tag{E10}$$

leading finally to the following:

$$E_T = \widehat{C}_E L_c \frac{\xi}{p} \left(\hat{e} - e_a + \Delta_{-T} T_\Delta + \Delta_\psi A \widehat{C}_E \delta_a + B T_\Delta \right) = \widehat{C}_E L_c \frac{\xi}{p} \left[(1 + \Delta_\psi A \widehat{C}_E) \delta_a + (\Delta_T + B) T_\Delta \right] \tag{E11}$$

Analogously to what was done in Section 2, we can now use the energy budget to obtain an expression for T_Δ. It is as follows:

$$R_A - 2\epsilon\sigma L_c T_a^3 T_\Delta = \underbrace{C T_\Delta}_{H} + \underbrace{\widehat{C}_E L_c \frac{\xi}{p} \left[(1 + \Delta_\psi A \widehat{C}_E) \delta_a + (\Delta_T + B) T_\Delta \right]}_{\lambda b E_T} + 2\epsilon\sigma L_c T_a^4 + L_c S_{nk} \tag{E12}$$

from the above Equation (E12), T_Δ can be singled out:

$$R_A = \left[C + \widehat{C}_E L_c \frac{\xi}{p} (\Delta_T + B) + 2\epsilon\sigma L_c T_a^3 \right] T_\Delta + \widehat{C}_E L_c \frac{\xi}{p} (1 + \Delta_\psi A \widehat{C}_E) \delta_a + 2\epsilon\sigma L_c T_a^4 + L_c S_{nk} \tag{E13}$$

and thus,

$$T_\Delta = \frac{R_a - \widehat{C}_E L_c \frac{\xi}{p} (1 + \Delta_\psi A \widehat{C}_E) \delta_a - 2\epsilon\sigma L_c T_a^4 - L_c S_{nk}}{C + \widehat{C}_E L_c \frac{\xi}{p} (\Delta_T + B) + 2\epsilon\sigma L_c T_a^3} \tag{E14}$$

After substitution of the temperature gap in Equations (3), (29) and (E11), we obtain the water-budget-aware thermal energy transport:

$$H = C \frac{R_a - \widehat{C}_E L_c \frac{\xi}{p} (1 + \Delta_\psi A \widehat{C}_E) \delta_a - 2\epsilon\sigma L_c T_a^4 - L_c S_{nk}}{C + \widehat{C}_E L_c \frac{\xi}{p} (\Delta_T + B) + 2\epsilon\sigma L_c T_a^3} \tag{E15}$$

the water-budget-aware water vapor gap is as follows:

$$e_\Delta = \hat{e} + \Delta_\psi A \widehat{C}_E \delta_a + (\Delta_T + B) \frac{R_a - \widehat{C}_E L_c \frac{\xi}{p} (1 + \Delta_\psi A \widehat{C}_E) \delta_a - 2\epsilon\sigma L_c T_a^4 - L_c S_{nk}}{C + \widehat{C}_E L_c \frac{\xi}{p} (\Delta_T + B) + 2\epsilon\sigma L_c T_a^3} \tag{E16}$$

and finally, the water-budget-aware transpiration rate is as follows:

$$E_T = C_E L_c \frac{\xi}{p} \hat{e} + \Delta_\psi A \widehat{C}_E \delta_a + (\Delta_T + B) \frac{R_a - \widehat{C}_E L_c \frac{\xi}{p} (1 + \Delta_\psi A \widehat{C}_E) \delta_a - 2\epsilon\sigma L_c T_a^4 - L_c S_{nk}}{C + \widehat{C}_E L_c \frac{\xi}{p} (\Delta_T + B) + 2\epsilon\sigma L_c T_a^3} \tag{E17}$$

The specific form of the above equations can be derived for the sun–shade model with a little further effort which we sketch below.

First, let us consider Equation (E7) with all the coefficients specialised for the sun-lit or shaded leaf. The subsequent calculation involves determining the equivalents of Equations (E10) and (E11). Then, these findings need to be substituted into the energy budgets Equation (33) and 34. It is important to note that the latter equations, in comparison to Equation (5), introduce two terms that create a coupling effect, resulting in a reciprocal dependence of the intermediate solutions. To simplify understanding these steps, consider the coupling terms as additional contributions to the sinks. Therefore, in Equation (32), where LcS_{nk} appears, substitute it with $L_{sh}S_{nk_{sh}} - 2\alpha_S \epsilon\sigma T_{Sun}^4$ for the shaded leaf temperature gap solution, and with $L_S S_{nk_S} - 2\alpha_{Sh} \epsilon\sigma T_{Sh}^4$ for the sunlit leaf temperature gap solution.

The coefficients α_S and α_{Sh} represent the fraction of longwave radiation received by shaded leaves from sunlit leaves and vice versa. Determining these coefficients remains an area for further research.